Tampere University

Katri Leino

IN VITRO DISSOLUTION OF POLYLACTIDE/BIOACTIVE GLASS COMPOSITES

Faculty of Engineering and Natural Sciences
Master of Science Thesis
Examiner: Associate Professor Jonathan Massera
Examiner: Professor Minna Kellomäki
Examiner: University Lecturer, Adjunct Professor Terttu Hukka
May 2020

ABSTRACT

Katri Leino: *In Vitro* Dissolution of Polylactide/Bioactive Glass Composites
Master of Science Thesis
Tampere University
Master's Degree Programme in Materials Science and Engineering
May 2020

Composite structures are an interesting area of study in the field of biomedical engineering. It is possible to customize the chemical properties of a bioactive glass and consequently the rate of both degradation and bonding to tissue. Whereas biocompatible polymers such as polylactide (PLA) are biodegradable, they do not bond with tissue as bioactive glasses do, but they do tend to have superior mechanical properties compared to glasses. Thus, by combining these two materials it is possible to create bioactive composites with tailored chemical properties and degradation rates that can be used in load-bearing tissue engineering applications.

The aim of this thesis was to investigate how bioactive glasses release ions through polymer matrix in composite structure and how different bioactive glasses react with the polymer matrix, changing the properties of the composite. The dissolution of pure PLA and six PLA/bioactive glass composites were studied during 10 weeks of *in vitro* hydrolysis in TRIS buffer at 37 °C. The composite rods were manufactured using either modified silicate glass 13-93 (10, 30, or 50 percentage by weight) or phosphate glass Sr50 (10, 25, or 35 percentage by weight). During the hydrolysis pH, mass loss, water absorption, ion release, glass content, and mechanical properties were studied.

During 10 weeks of hydrolysis, no substantial changes in pH, mass or mechanical properties of the pure PLA were observed. Composites with the lowest glass content (10%) showed little difference compared with the pure PLA, however an increase in the glass content induced changes in solution pH, sample mass and water uptake. It was shown that the glass particles dissolve through the polymer matrix. As expected, the phosphate glass dissolved faster than the silicate glass and composites degraded faster than pure PLA. Enhanced degradation rate of the composites was manifested by higher weight loss and decrease in mechanical properties. The results also indicate that the higher the glass content in the composite, the more the mechanical properties of the composite decrease and the faster the glass dissolves. The degradation of PLA/bioactive glass composites is greatly dependent on the type of glass used as filler and the amount of glass used.

Keywords: polylactide, bioactive glass, composite, *in vitro*, degradation

TIIVISTELMÄ

Katri Leino: Polylaktidi-bioaktiivinen lasi -komposiittien *in vitro* -hajoaminen
Diplomityö
Tampereen yliopisto
Materiaalitekniikan diplomi-insinöörin tutkinto-ohjelma
Toukokuu 2020

Komposiittirakenteet ovat mielenkiintoinen tutkimuskohde biolääketieteen saralla. Bioaktiivisten lasien kemiallisten ominaisuuksien räätälöinti mahdollistaa sekä hajoamisnopeuden että kudossidosten muodostumisnopeuden muokkaamisen kuhunkin sovellutukseen soveltuvaksi. Vaikka bioyhteensopivat polymeerit, kuten polylaktidi (PLA), ovat biohajoavia, eivät ne muodosta sidoksia kudoksen kanssa, mutta niillä on tyypillisesti kuitenkin paremmat mekaaniset ominaisuudet kuin lasilla. Täten yhdistämällä nämä kaksi komponenttia on mahdollista luoda räätälöityjä bioaktiivisia komposiitteja, joiden hajoamisnopeus ja kemialliset ominaisuudet ovat tarkasti tiedossa, ja joita voidaan käyttää myös mekaanisesti haastaviin kudosteknologisiin sovellutuksiin.

Tämän diplomityön tarkoitus oli tutkia miten bioaktiiviset lasit vapauttavat ioneja komposiittirakenteisen polymeerimatriisin läpi sekä miten erilaiset bioaktiiviset lasit reagoivat polymeerimatriisin kanssa aiheuttaen muutoksia komposiitin ominaisuuksiin. Puhtaan PLA:n sekä kuuden PLA-bioaktiivinen lasi -komposiitin liukenemis- ja hajoamiskäyttäytymistä selvitettiin 10 viikon *in vitro* -tutkimuksessa. Komposiittisauvat sisälsivät joko modifioitua 13-93-silikaattilasia (10, 30 tai 50 painoprosenttia) tai Sr50-fosfaattilasia (10, 25 tai 35 painoprosenttia). Hydrolyysitutkimus suoritettiin 37-asteisessa TRIS-puskuriliuoksessa ja tutkittavia parametrejä olivat pH, massan muutos, vedensitomiskyky, ionien vapautuminen, lasipitoisuus sekä mekaaniset ominaisuudet.

10 viikon aikana puhtaan PLA:n pH, massa tai mekaaniset ominaisuudet eivät muuttuneet. 10 % lasia sisältävät komposiitit eivät juurikaan eronneet tuloksissaan PLA:sta. Komposiitin lasipitoisuuden lisääntyessä erot kuitenkin tulivat selvemmiksi pH:n, massan ja vedensitomiskyvyn osalta. Saadut tulokset osoittavat, että lasipartikkelit liukenevat polymeerimatriisin läpi ja odotetusti fosfaattilasi liukeni nopeammin kuin silikaattilasi. Mekaanisten ominaisuuksien heikkeneminen sekä suurempi vedenottotaipumus ovat todisteita siitä, että komposiitit hajoavat nopeammin kuin puhdas polymeeri. Tulosten perusteella voidaan myös sanoa, että mitä enemmän komposiitissa on lasia ennen hydrolyysikokeen aloitusta, sitä enemmän sen mekaaniset ominaisuudet heikkenevät ja sitä nopeammin lasi liukenee. Yhteenvetona voidaan sanoa, että PLA-bioaktiivinen lasi -komposiittien hajoaminen riippuu suuresti käytetystä lasityypistä sekä käytetyn lasin määrästä.

Avainsanat: polylaktidi, bioaktiivinen lasi, komposiitti, *in vitro*, hajoaminen

PREFACE

The experimental part of this study was carried out in the Biomaterials and Tissue Engineering Group of the Institute of Biosciences and Medical Technology (BioMediTech) at Tampere University of Technology (TUT) in year 2017. The SEM experiments were carried out in the Work Environment Laboratories of Finnish Institute of Occupational Health in year 2017.

I want to thank Associate Professor Jonathan Massera, Professor Minna Kellomäki and University Lecturer, Adjunct Professor Terttu Hukka for offering me the possibility to participate in this interesting study and for the amount of knowledge and support I was provided with. In addition, I want to express my gratitude to MSc (Tech.) Inari Lyyra for her help and guidance both in and outside the laboratory. I also want to acknowledge the whole Biomaterials and Tissue Engineering research group for providing a friendly and inspiring working environment.

I am also grateful to both my husband and friends for their patience and support during this long process, thank you.

Tampere, 26.4.2020

Katri Leino

CONTENTS

LIST OF ABBREVIATIONS AND SYMBOLS

13-93	certain bioactive silicate glass
Ag	silver
Al_2O_3	aluminium oxide; alumina
Au	gold
BioMediTech	Institute of Biosciences and Medical Technology
BO	bridging oxygen
Ca	calcium
Ca^{2+}	calcium ion; cationic form of atomic calcium
CaO	calcium oxide; quicklime; burnt lime
CaP	calcium phosphate
CH_3	methyl group
Cu	copper
DI	deionised
F	fluorine
GPC	gel permeation chromatography
H	hydrogen
H^+	hydron; proton; cationic form of atomic hydrogen
H_2O	water
H_3O^+	hydronium; hydroxonium; hydrated form of hydrogen cation
HA	hydroxy apatite
HCA	hydroxycarbonate apatite
HPO_4^{2-}	hydrogen phosphate
ICP	inductive coupled plasma
K	potassium
K^+	potassium ion; cationic form of atomic potassium
K_2O	potassium oxide; potash
M	glass network modifier
Mg	magnesium
Mg^{2+}	magnesium ion; cationic form of atomic magnesium
MgO	magnesium oxide; magnesia
mol%	molecular percentage
MPa	megapascal; unit of stress (N mm^{-2})
Na	sodium
Na^+	sodium ion; cationic form of atomic sodium
Na_2O	sodium oxide
NBO	non-bridging oxygen
OES	optical emission spectrometry
OH	hydroxyl group
OH^-	hydroxide
P	phosphorus
P_2O_5	phosphorus pentoxide
PO_4^{3-}	phosphate
ppm	parts per million
SEM	scanning electron microscopy
Si	silicon
SiO_2	silicon dioxide; silica
SiO_4	silicate
$Si(OH)_4$	silicic acid

Sr	strontium
Sr^{2+}	strontium ion; cationic form of atomic strontium
Sr50	certain bioactive phosphate glass
SrO	strontium oxide; strontia
PLA	polylactide
rpm	revolutions per minute
RT	room temperature
T_g	glass transition temperature
TGA	thermogravimetric analysis
TiO_2	titanium dioxide; titania
T_m	melting temperature; melting point
TRIS	tris(hydroxymethyl)aminomethane
TUT	Tampere University of Technology
wt%	percentage by weight; weight percent
Zn	zinc

1. INTRODUCTION

A bioactive material is defined as "a material that elicits a specific biological response at the interface of the material which results in the formation of a bond between the tissues and the material". Motion between the tissue and the bioactive material is prevented by the interfacial bond and this mimics the interface that is formed when natural tissues repair themselves. The bioactive concept includes many materials with a wide range of bonding rates and thickness of interfacial bonding layers. These materials include bioactive glasses, bioactive glass-ceramics, dense synthetic hydroxy apatite (HA), bioactive composites, and bioactive coatings. All these materials form an interfacial bond with bone, in some cases also with soft tissue, but the time dependence of bonding, bond strength, bonding mechanism, bonding zone thickness, mechanical strength, and fracture toughness differ. A common characteristic of all bioactive materials is the formation of a hydroxycarbonate apatite (HCA) layer on their surface when implanted into biological environment. The composition and structure of the HCA phase is equivalent to the mineral phase of bone. [1, p. 49; 2, pp. 5–9; 3–5]

What sets bioactive glasses apart from other bioactive ceramics and glass-ceramics is the possibility of controlling its chemical properties and thus the rate of both degradation and bonding to tissue. It is possible to design glasses with properties specific to a particular clinical application by using different components to form the glass network or by adding therapeutic ions. [1, p. 49; 6] Biocompatible polymers such as polylactide (PLA) are biodegradable. Yet, they do not bond with tissue as bioactive glasses do, but they do tend to have superior mechanical properties compared to glasses. Thus, by combining these two materials it is possible to create bioactive composites with tailored chemical properties and degradation rates that can be used in load-bearing tissue engineering applications. [7–9]

This thesis is a continuation of a previous study [10]. The aim of this work is to investigate how different bioactive glasses (phosphate glass Sr50 and modified version of silicate glass 13-93) release ions through polymer matrix in composite structure and how different bioactive glasses react with the polymer matrix, thus changing the properties of the composite. The *in vitro* degradation of PLA and six PLA/bioactive glass composites were studied during 10 weeks of hydrolysis. Also, some previously unanalysed composite specimens from the previous study were analysed for this thesis. The parameters studied in this work were the pH of the buffer solution, water absorption and mass loss of the sample rods, ion release to the buffer solution, thermogravimetric analysis and scanning electron microscopy imaging of the sample rods, as well as bending and shear strength of the sample rods.

2. POLYLACTIDE

Polylactide (PLA) is a biocompatible and biodegradable aliphatic polyester that can be manufactured from renewable resources. PLA has a broad field of applications such as agricultural films, packing, automotive industry, garments, biodegradable fibres, biomedical devices, and recyclable wood/plastic composites. [11–13]

2.1 Structure, properties and applications

PLA (Figure 1) can be produced either by condensation polymerisation from lactic acid (2-hydroxy propionic acid) or via ring-opening polymerisation of cyclic dimer, lactide. Polycondensation of PLA yields only low to intermediate molecular weight polymer and in this process the stereoregularity of the polymer can be controlled poorly. The ring-opening polymerisation enables production of high molecular weight polymer with better control over stereoregularity. Production of PLA via azeotropic dehydration condensation is also possible but this method is not that commonly used. Polymer manufactured by condensation polymerisation is often referred as poly(lactic acid) and polymer produced by ring-opening polymerisation is called polylactide. These are essentially the same polymer and they are both abbreviated PLA. [13; 14, pp. 278–279; 15, p. 71–97 & 143–144; 16, p. 155; 17]

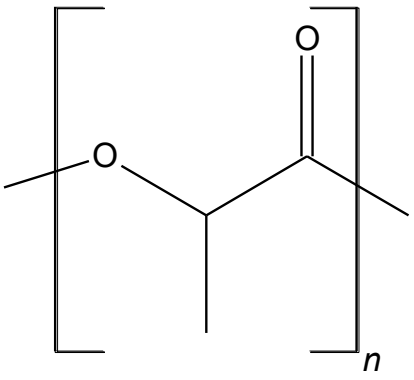

Figure 1. *Structure of the repeating unit of polylactide (PLA), adapted from [18, p. 394].*

PLA is a thermoplastic, aliphatic linear polyester. PLA is optically active and it can be found in three stereoisomeric forms: poly-L-lactide (PLLA), poly-D-lactide (PDLA), and racemic poly-D,L-lactide (PDLLA) as shown in Figure 2. In nature, mammals can produce only the L-form, whereas bacteria can produce both L- and D-forms. [13; 14, pp. 278–297; 15, pp. 71–97 & 143–144; 19] Even though properties of PLA depend on the component isomers, processing temperature, annealing time and molecular weight, in

general it is considered to have high mechanical strength and modulus, be biodegradable, biocompatible, bioabsorbable and to exhibit low toxicity as well as being easy to process. [11, 20]

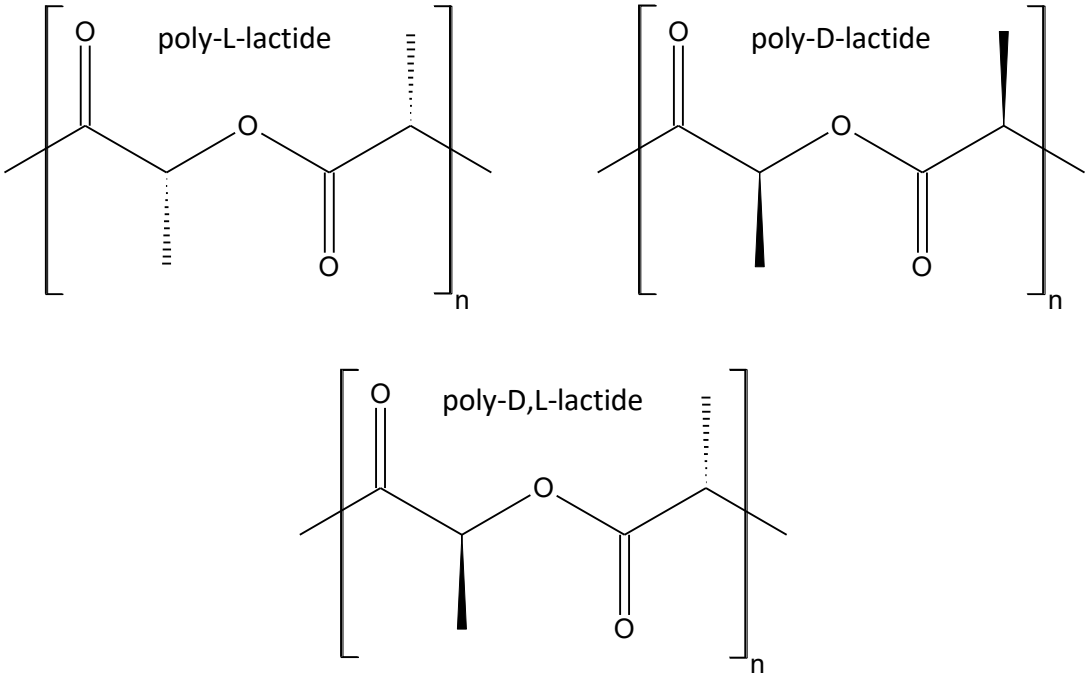

Figure 2. *Stereoisomers of polylactide (PLA), adapted from [13].*

Both PLLA and PDLA are semicrystalline polymers having glass transition temperature (T_g) of about 55 °C and melting temperature (T_m) of circa 175 °C. The degradation period of PLLA and PDLA in aqueous environment is quite long, typically minimum of two years. As all of the methyl groups (-CH_3) of PLLA and PDLA are on the same side, the polymer chains can pack tightly, and this results in rather stable structure. Racemic PDLLA (T_g about 55–60 °C) has a randomly alternating arrangement of methyl and hydrogen (-H) groups, which prevents the polymer chains from packing tightly. As a result of this, the polymer is amorphous and has lower mechanical strength and shorter degradation period (typically 9–12 months) in aqueous environment. [7, 8, 12, 13, 19]

The crystallinity of PLA can be decreased by using different monomers as copolymers (for example adding L-lactide into PDLA) as they work as defects in the structure of the polymer and disrupt the formation of the highly organised crystals. The degree of crystallinity and orientation affect the tensile properties of the material: the mechanical properties improve with growing organisation in the structure. The methyl groups in PLA makes it slightly hydrophobic and thus its water absorption and degradation rate are quite slow. [7, 8, 12, 20–22]

Due to its good mechanical properties PLLA has been regarded as an ideal material for load bearing biomedical applications whereas lower mechanical strength and relatively fast degradation rate make PDLLA interesting for example for drug delivery applications. [7, 23]

2.2 Hydrolytic degradation

PLA can degrade due to irradiation, thermal-, mechanical- or chemical stress, enzymatically, microbiologically, or via hydrolysis. The degradation rate of PLA is dependent on range of factors, such as molecular weight, crystallinity, purity, and water permeability. PLA degrades into normal human metabolic by-product, lactic acid, which is further broken down into water and carbon dioxide by the citric acid cycle. [14, p. 271; 20]. In this thesis only hydrolytic degradation is discussed in detail as that is the only relevant degradation method in the scope of this work.

Like other polyesters, also PLA is susceptible to hydrolytic degradation. PLA can be degraded in aqueous environment by simple hydrolysis of the ester bond (see Figure 3). The first step in the hydrolysis of PLA is water absorption into the polymer matrix. The process continues by chain scission of the hydrolytically unstable ester bonds in the polymer backbone where the chain scission can occur either via random scission or chain end scission. The increasing number of acidic chain ends being formed during the degradation accelerate the cleavage of the chemical bonds in the polymer backbone via chain end scission. Since the hydrolysis of PLA results in the formation of hydroxyl and carboxylic end groups, the reaction is autocatalytic and there is no need for presence of enzymes to catalyse this hydrolysis. [12–13; 14, p. 271; 21]

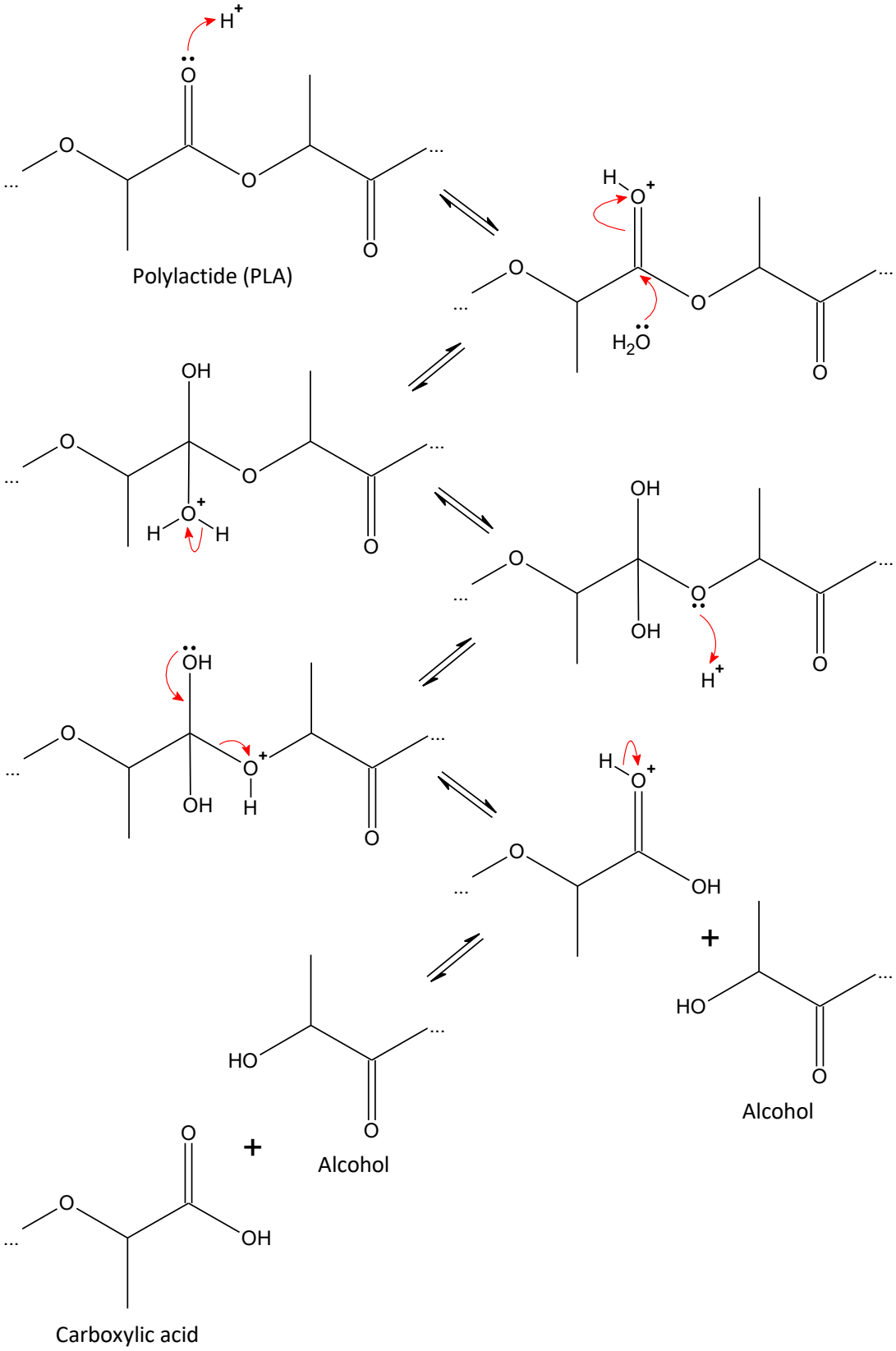

Figure 3. *Hydrolysis of PLA in acidic conditions, adapted from [12; 24; 25, p. 209]. The hydrolysis starts with water absorption into the polymer matrix and continues by chain scission of the labile ester bonds in the polymer backbone.*

In general, the hydrolytic degradation of biodegradable polymers can occur via surface or bulk erosion. PLA however is a bulk-eroding polymer. Bulk erosion results into homogenous degradation throughout the material and the primary reason for this is diffusion of water into the polymer matrix. For bulk-eroding polymers the water absorption is faster than the degradation of the polymer bonds and therefore the degradation is not limited to the polymer surface. [26, 27]

The hydrolytic degradation rate of both PLLA and PDLA is quite slow, as it may take years for these to fully hydrolyse. Racemic PDLLA as well as copolymers of PLLA and PDLA have faster hydrolytic degradation rate, and these are typically hydrolysed within 12 months. [7, 8, 13]

3. BIOACTIVE GLASSES

In 1971 Hench published an article demonstrating that bone can bond to certain silicate glass compositions. These bioactive glasses were the first synthetic materials to demonstrate bonding to bone, and they have been effectively used for bone regeneration since then. Instead of being inert like a window glass, bioactive glasses interact with tissue, resulting in the formation of a strong interfacial bond between the bone and the glass. Bioactive glasses can degrade in the body at a rate matching that of bone formation. Through a combination of apatite crystallisation on their surface and controlled release of therapeutically active ions they stimulate bone cell proliferation, which results in bone regeneration rather than replacement, thereby restoring the original bone state and function. Phosphate glasses are relatively new and less studied type of bioactive glass compared to silicate glasses but their solubility, which can be customized by changing the glass composition and ranges over several orders of magnitude, makes them a promising class of biomedical materials. [3, 6, 28, 29]

3.1 Structure, properties and applications

Glass is amorphous with a continuous, random network having no long-range order. The glass network is usually composed of three different components: network formers, network modifiers and intermediate oxides (Figure 4). Network formers (for example silica (SiO_2) and phosphorus pentoxide (P_2O_5)) link together through bridging oxygens and can form glasses without the need for additional components. Glasses having a SiO_2 backbone are called silicate glasses and glasses based on P_2O_5 are called phosphate glasses. Network modifiers (typically oxides of alkali or alkali earth metals such as sodium (Na), calcium (Ca), and potassium (K)) alter the glass structure by turning bridging oxygen (BO) atoms into non-bridging oxygen (NBO) atoms. Intermediate oxides (such as titania (TiO_2) and alumina (Al_2O_3)) can either act like network modifiers or may possibly enter the backbone of the glass structure, acting more like network formers. Therapeutic ions such as strontium (Sr), zinc (Zn) or fluoride (F) can be incorporated into the glass to be released upon degradation for stimulation of bone growth, wound healing, and for prevention of infections. [2, pp. 18–19; 6, pp. 45–47; 29; 30, pp. 464–465]

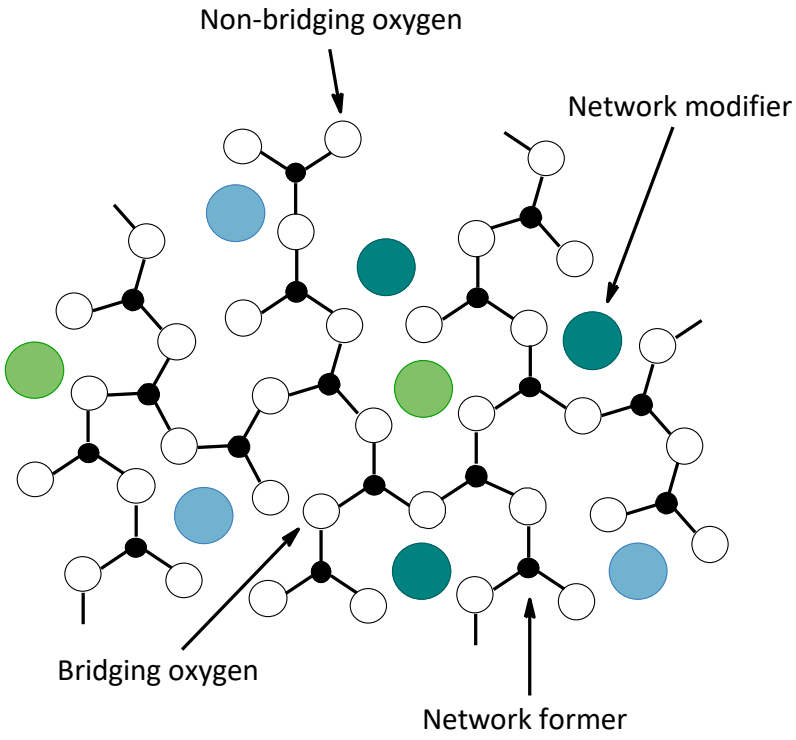

Figure 4. *Schematic structure of a bioactive glass. The network is composed of network formers, network modifiers, and both bridging and non-bridging oxygens. Adapted from [2, p. 18; 30, p. 465; 31].*

The fundamental building unit of silicate glasses is the silicate (SiO_4) tetrahedron, which can be connected to neighbouring SiO_4 tetrahedra through covalent Si-O-Si bonds (bridging oxygens). In vitreous silica, each tetrahedron is linked to other tetrahedra at each of its four corners, which corresponds to four BOs per tetrahedron. In silicate glass the network modifiers (M) turn BOs into NBOs by forming Si-O-M^+ linkages. Glasses with up to approximately 53 mole percent (mol%) of SiO_2, not only develop a bond with bone but also form an adherent, interdigitating collagen bond with soft tissues. Glasses with SiO_2 content of 53–58 mol% are bioactive, but only bond to bone. Glass compositions with over 60 mol% of SiO_2 do not bond with tissue. [1, p. 61; 2, pp. 18–19; 6]

The glass-forming component in phosphate glasses is P_2O_5, and orthophosphate (PO_4^{3-}) tetrahedron is the basic unit in the phosphate glass structure. As the phosphorus is connected to one of the oxygen atoms by a double bond, only three oxygen atoms can bond to other PO_4^{3-} by covalent P-O-P bonds (bridging oxygens). Pure P_2O_5 glass is very reactive and hygroscopic, and is only of scientific interest. In practical applications, the durability of the glass is increased by adding network modifiers that form ionic P-O-M^+ linkages. Phosphate glasses can be arranged under four categories based on their P_2O_5 content: ultraphosphate glasses (more than 50 mol% P_2O_5), metaphosphate glasses (50

mol% P_2O_5), polyphosphate glasses (less than 50 mol% P_2O_5), and pyrophosphate glasses (less than 33.3 mol% P_2O_5) [6; 29, pp. 45–48; 31]

The addition of network modifier oxides (such as sodium oxide (Na_2O) and calcium oxide (CaO) to the glass results in the cleavage of BO bonds and the creation of NBOs in the glass structure. The subsequent glass structure is disrupted, comprised not only covalent Si-O-Si (in silicate glasses) or P-O-P (in phosphate glasses) bonds but also ionic cross-linkages between NBOs. This process is called depolymerisation of the glass network. The BOs between network formers hold the network together, and NBOs between network formers and modifier ions disrupt the network and modify the properties of the glass. The biological behaviour of glasses depends on the relative proportion of BO bonds to NBO bonds in the phases of the material. Glass properties, such as stability against hydrolytic attack, crystallisation tendency, mechanical properties, and degradation rate depend not only on the phosphate or silica content but also on the charge-to-size ratio of the network modifier cations, which determines how strong the ionic cross-links between two NBOs are. [2, pp. 18–19; 29, pp. 45–50; 31; 32, p. 65]

Most clinical applications of bioactive glasses associate to the repair of the skeletal system where the glass solubility must be meticulously controlled in order to match the resorption rate of the implant to the rate of bone growth. In many applications glasses and ceramics are used as implants but they can be also used as coatings on a substrate, or as a second phase in a composite. By making sintered porous scaffolds or glass fibres, substrates for a range of biomedical applications can be produced. [2, pp. 1–4; 29, p. 62] The primary drawback of bioactive glasses is its brittle nature and low fracture toughness [1, p. 53]. Not even the A-W glass-ceramic possessing the highest mechanical strength among bioceramics can replace highly loaded bones such as tibial and femoral bones. Therefore, development of bioactive materials such as composites with mechanical properties equivalent to those of the natural bone is needed. [33]

Bioactive glasses and ceramics are also used for soft tissue applications such as engineering of ligaments, muscle or cartilage regeneration, and replacement parts of the cardiovascular system, especially heart valves. In addition, it has been proposed that degradable phosphate glasses could possibly be used for neural repair and nerve regeneration [34]. The bioactive glasses capability to release ions upon degradation can also be utilized in the development of materials for controlled release of therapeutically active ions for the treatment of tumours and osteoporosis, or for release of antibacterial ionic species such as copper (Cu), zinc (Zn), or silver (Ag). [2, pp. 1–4; 29, pp. 62–63; 35]

3.2 Degradation in aqueous solution

The bioactive glasses bonding with bone is based on the chemical reactivity of the glass in body fluids, which results in the dissolution of the glass and formation of a biologically active hydroxycarbonate apatite (HCA) layer to which bone can bond. The tissue bonding

rate of the glass seems to depend on the rate of HCA formation. Both the rate of dissolution and kinetics of the reaction stages are highly dependent on the glass composition. [1, p. 54]

3.2.1 Silicate glass dissolution

Upon immersion of a bioactive silicate glass in an aqueous solution, three overall processes occur: leaching, dissolution, and precipitation. Leaching is characterised by release of alkali and alkali earth metal ions such as Na^+, K^+, and Ca^{2+}. Na^+ and K^+ are usually released by ion exchange with H^+ (or H_3O^+) ions of the solution whereas cations such as Ca^{2+} and Sr^{2+} are merely released into the solution. Leaching is quite easy and fast as modifier cations are not as strongly bonded as the silicate network, and this process is usually controlled by diffusion. The ion exchange process leads to an increase in the interfacial pH (to values above 7.4). [1, p. 54; 5; 36; 37]

Network dissolution occurs simultaneously with the leaching as water breaks the soluble Si-O-Si bonds. Breakdown of the network occurs locally and releases silica into the solution in the form of silicic acid ($Si(OH)_4$). The hydrated silica (SiOH, silanol) formed on the glass surface by these reactions is rearranged by polycondensation of neighbouring silanols, resulting in a gel layer rich in silica. As alkali and alkali earth metals leach out of the bulk glass first, and the SiO_2 network degrades locally, silicate glass dissolution is said to be non-congruent. [1, p. 54; 5; 36–38]

In the precipitation reaction, Ca^{2+} and PO_4^{3-} released from the silicate glass, in addition to those in the solution, create a layer rich with calcium phosphate (CaP) on the surface of the glass. *In vitro* formation of the CaP layer occurs mainly on top of the silica gel, while *in vivo* it is formed inside the silica gel layer. Initially the CaP phase accumulating in the gel surface is amorphous. Later it crystallises to a HCA structure by including carbonate anions from the solution in the amorphous CaP phase. The nucleation and growth mechanism of the HCA layer seems to be the same both *in vivo* and *in vitro*, and it is accelerated by the presence of SiOH. [1, pp. 54–55; 4; 5]

3.2.2 Phosphate glass dissolution

In aqueous solution phosphate glasses can dissolve entirely, forming non-toxic ionic species normally found in the human body. For the readily occurring dissolution of ultraphosphate glasses and vitreous P_2O_5, cleavage of P-O-P bonds is necessary. But for meta- and polyphosphate glass dissolution, no P-O-P bond cleavage is necessary. Bioactive phosphate glasses dissolve via hydration of whole phosphate chains and subsequent chain disentanglement and dissolution, and for this reason phosphate glass dissolution is said to be congruent. This can be observed by comparing phosphate chain lengths in the glass and those found in the solution: the phosphate chains stay intact during glass dissolution.

After the initial hydration and dissolution, hydrolysis of polymeric phosphate chains follows in the solution, but at a considerably slower rate. [29, pp. 45 & 56; 31; 34; 38]

As with all bioactive glasses, also phosphate glass dissolution rate is extremely sensitive to the composition of the glass. In general, solubility increases with increasing P_2O_5 content. When phosphate glasses dissolve, their effect on the pH of the surrounding solution is different than with silicate glasses. Phosphate glasses give an acidic pH due to the gradual breakdown of phosphate chains that gives acidic species such as HPO_4^{2-} and PO_4^{3-} in the solution. By decreasing the phosphate content, the pH change can be increased towards neutral. Phosphate glass dissolution increases dramatically in acidic environment, but an alkaline pH also increases glass dissolution, even if at a slower rate. Therefore, if glass degradation needs to be controlled, it is important to maintain the pH in a neutral range. Phosphate glass dissolution is an autocatalytic process because upon initial degradation of the phosphate glass the local pH is lowered and the glass will subsequently be dissolved faster, as its degradation rate increases with decreasing pH. [29, pp. 57–58; 31; 38; 39]

4. COMPOSITES

The basic requirements for a material used in biomedical applications are biocompatibility, biodegradability, and appropriate mechanical properties. For instance, a multifunctional material for bone tissue regeneration should induce new bone tissue formation without an addition of organic bone growth factors, induce new blood vessel formation, degrade gradually at a rate matching the regeneration of new bone, and have antibacterial and anti-inflammatory activity. These complex functions can be achieved with multicomponent materials, composites. [8, 40]

4.1 Structure, properties and applications

A composite material (Figure 5) can be defined as a mixture of two or more phases whose mechanical performance and other properties surpass the constituent materials. One of the phases is called the reinforcement and it is typically discontinuous, stronger, and stiffer than the continuous phase that is called the matrix. The matrix is usually less stiff and weaker than the reinforcement phase. Due to chemical interactions and/or other processing effects, sometimes an additional and separate phase called an interphase is formed between the matrix and the reinforcement. [41–42; 43, pp. 7 & 73; 44, p. 1]

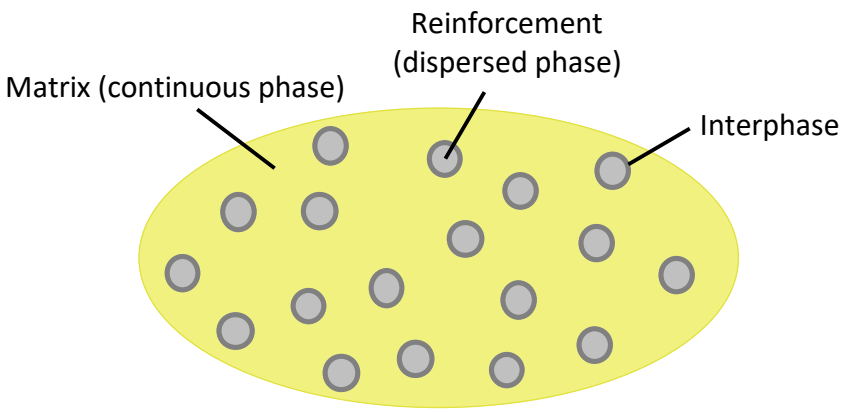

Figure 5. *Phases of a composite material. Adapted from [44, p. 1].*

The properties of a composite material are dependent on the properties and geometry of the components as well as the distribution of the phases. In principle, composites can be manufactured from any material, but components can be broadly grouped into three categories: polymers, metals, and ceramics. In Table 1, there are some performance rankings of materials used as composite components. Polymers, metals and ceramics are widely used matrix materials, but all of these can also be used as reinforcement phases e.g. as fibres, particles, flakes or sheets (Figure 6). [41; 44, pp. 1 & 18]

Table 1. *Structural performance ranking of conventional materials. Symbols: ++ = superior, + = good, – = poor, v = variable. Adapted from [44, p. 19].*

Property	Metals	Bulk ceramics	Fibre ceramics	Polymers
Tensile strength	+	–	++	v
Stiffness	++	v	++	–
Fracture toughness	+	–	v	+
Impact strength	+	–	v	+
Density	–	+	+	++
Dimensional stability	+	v	+	–
Thermal stability	v	+	++	–
Hygroscopic sensitivity	++	v	+	v
Erosion resistance	+	+	+	–

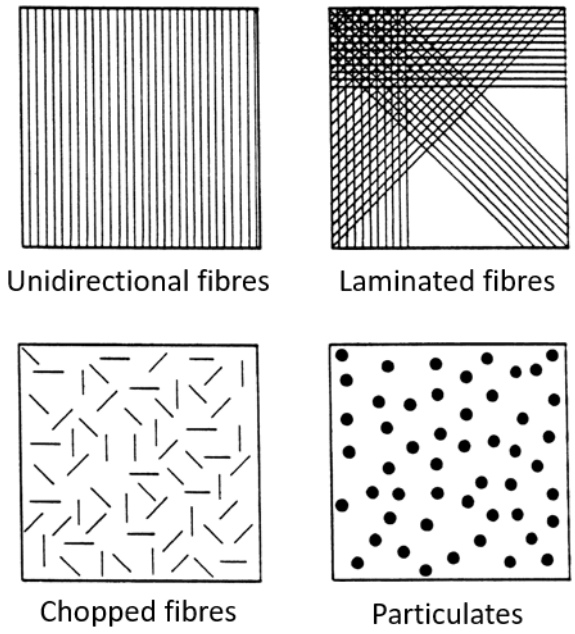

Figure 6. *Examples of reinforcement phases in composites. Adapted from [42].*

The composite phases play different roles depending on the application and type of the composite material. In low- to medium-performance composites the reinforcement, typically incorporated as particles or short fibres, may stiffen the structure to a certain degree but can only provide limited strengthening of the material. The matrix is the principal load-bearing component usually controlling the mechanical properties of the material. In high-performance composites, the typically continuous fibre reinforcement is the backbone of the material determining the stiffness and strength of the composite in the fibre

direction. The matrix phase delivers protection for the sensitive fibres, bonding, support, and local stress transfer from one fibre to another. Though small in dimensions, the interphase can play a critical role in controlling the failure mechanisms, failure spread, fracture toughness, and the overall stress-strain behaviour to failure of the material. [44, p. 2]

Two-phase composite materials are classified into three general groups depending on the type, orientation, as well as geometry of the reinforcement phase. These categories are particulate composites, discontinuous or short-fibre composites, and continuous-fibre composites. Particulate composites are comprised of particles with variety of sizes and shapes that are randomly dispersed inside the matrix. Short-fibre composites have short fibres, nanotubes, or whiskers as the reinforcing phase. These short fibres, which can be quite long compared to their diameter, can be either randomly oriented or oriented in a specific direction. The most effective from the viewpoint of stiffness and strength are the continuous-fibre composites, reinforced by long continuous fibres. The continuous fibres can all be parallel (unidirectional continuous-fibre composite), oriented at right angles to each other (cross ply or woven fabric continuous-fibre composite), or oriented along numerous directions (multidirectional continuous-fibre composite). [44, pp. 24–25]

As polymers in general, also biodegradable polymers typically have good processing qualities. While polymers have inadequate interaction with tissue, bioactive glasses stand out in biological performance. As a drawback, glasses are difficult to process. If these two components are used together to form a composite, it is possible to gain an easily processable material with a wide range of chemical and biological properties. Composites used in biomedical applications are typically comprised of a biodegradable polymer matrix (usually poly(lactide-*co*-glycolide) or PDLLA) and a bioactive glass reinforcement phase, which is incorporated to the matrix either as particulates or as fibres. Other possible biomedical composite approaches include coating porous glass structures with biodegradable polymers or coating a biodegradable polymer scaffold with bioactive glass particles. Polymer matrix is used to utilize the processability and elasticity of the polymeric component while increasing the bioactivity and stiffness of the structure with bioactive glass. The reason why bioactive glasses are attractive composite modifiers is the chance to control a variety of chemical and biological properties by tailoring the chemistry and structure of glasses by varying composition, preparation method, and manufacturing conditions. [8, 40, 45–47]

Volume fractions of the phases along with the size, shape and distribution of the reinforcement material have significant effects on the biological and mechanical properties of the composite. For instance, when the particle size of bioactive glass is reduced or more glass is added to the structure, the bioactivity of the composite increases. However, this leads to a larger interfacial area between the polymer and the glass, which may reduce crack resistance. The mechanical properties are also greatly affected by the interface between different phases, thus good interfacial bonding is preferred. The uniformity of the

composite is determined by the distribution of the reinforcement phase. The more nonuniform the reinforcement distribution, the more heterogeneous the material, and the wider the distribution in properties and the probability of failure in the weakest areas. [8; 40; 44, pp. 1–2; 45]

Uses of composites are plentiful, including aircraft, aerospace, automotive, marine, infrastructure, energy, armour, sports as well as biomedical applications. Biomedical applications of composites include artificial limb parts and prosthetic devices. Biodegradable polymer/bioactive glass composites have great potential in biomedical applications, especially in tissue engineering, regenerative medicine and drug delivery systems. [40; 44, pp. 3 & 10]

4.2 Degradation of biodegradable polymer/bioactive glass composites

Bioactive glass affects the degradation behaviour of the polymer matrix thus resulting into the composite's different dissolution behaviour compared to the constituent materials' dissolution behaviour. The degradation behaviour of biodegradable, bioactive polymer-based composites can be controlled not only by altering the amount of bioactive glass reinforcement but also the composition, specifically the amount of alkaline network modifiers (e.g. CaO). [40, 48]

Bioactive glass increases the hydrophilicity and wettability of the composite structure, which can result in higher levels of water absorption and increase in the surface area of hydrolytic attack resulting in an increased degradation rate. Greater quantity and smaller particle size of the bioactive glass leads to more rapid degradation of the composite. A delayed degradation of the composite can be accomplished by the buffering effect caused by dissolution of basic ions (e.g. Ca^{2+} or Na^{+}) from the bioactive glass structure. This causes the acidic by-products released by the of the polymer degradation to be neutralized and therefore the autocatalytic degradation process is hindered. The possibly dissimilar degradation rates of different phases in the composite system can lead to apprehensions about the potential instability of the structure after implantation. [8, 40, 45, 49–51]

5. MATERIALS AND METHODS

5.1 Test specimen preparation

In this study, medical grade poly(L-lactide-*co*-D,L-lactide) 70:30 (RESOMER® LR 706 S, Evonik Industries AG, Darmstadt, Germany) was used to prepare the polymer rods and the polymer/bioactive glass particulate composites. Inherent viscosity of the polymer (as reported by the manufacturer) was 4.10 dl g^{-1}. The bioactive glasses used in the study were modified silicate glass 13-93 and phosphate glass Sr50. The compositions of these glasses in molecular percentage (mol%) are shown in Table 2.

Table 2. *Compositions in molecular percentage (mol%) of the bioactive glasses 13-93 (modified) and Sr50 used in this study.*

Glass	SiO_2 (mol%)	P_2O_5 (mol%)	CaO (mol%)	Na_2O (mol%)	MgO (mol%)	K_2O (mol%)	SrO (mol%)
13-93	54.6	1.7	22.1	8.0	7.7	5.9	-
Sr50	-	50.0	20.0	10.0	-	-	20.0

The rods (diameter approximately 2 mm) made from pure PLA, PLA+13-93, and PLA+Sr50 were manufactured as part of a previous study [10] with a co-rotating twin-screw extruder (Mini ZE 20*11.5 D, Neste Oy, Porvoo, Finland) under nitrogen atmosphere. The PLA+13-93 composites contain 10, 30, or 50 percentage by weight (wt%) bioactive glass 13-93 and the PLA+Sr50 composites 10, 25, or 35 wt% bioactive glass Sr50. The particle size for both glasses is 125–250 µm. The rods were cut to 7-cm test specimens (see Figure 7) for the *in vitro* hydrolysis (see chapter 5.2).

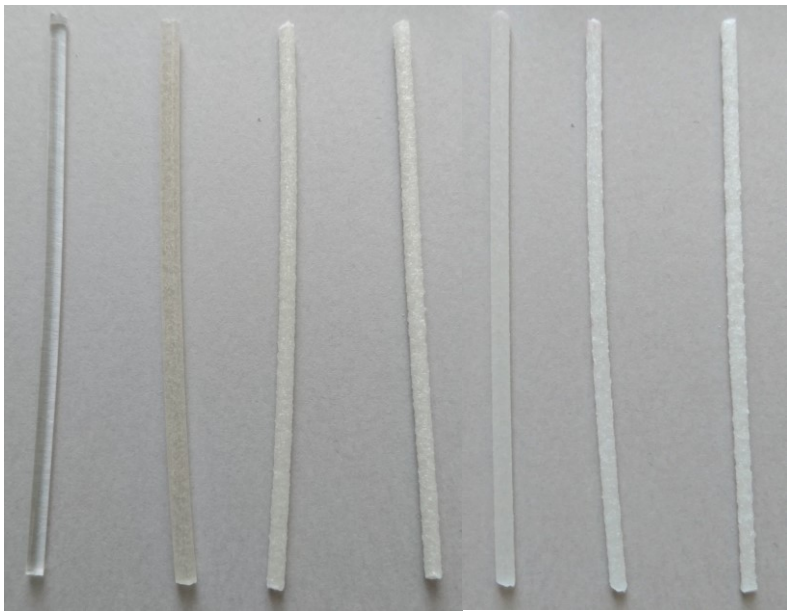

Figure 7. *One set of test specimens used in the in vitro hydrolysis study. From left: PLA, PLA+13-93 10/30/50%, and PLA+Sr50 10/25/35%. Sample length 7 cm and diameter ca. 2 mm.*

Three parallel sets of test specimens were prepared for each time point of the hydrolysis study.

5.2 *In vitro* hydrolysis

The *in vitro* degradation properties of the pure PLA and each of the six composites were studied using three parallel sets of specimens. One set of these specimens can be seen in Figure 7. The hydrolyses were conducted in 13 ml plastic test tubes equipped with tight caps. Test tubes, caps, and test specimens were rinsed with ethanol (96% GPR RECTA-PUR, VWR Chemicals) and left to dry in a laminar hood prior to use. Dry test specimens were weighed on an analytical scale (Mettler Toledo AB265-S/FACT and Mettler Toledo AG245, Mettler-Toledo International Inc., Greifensee, Switzerland) before hydrolyses were started.

For the dissolution studies, several batches of 0.05 M tris(hydroxymethyl)aminomethane (TRIS) buffer solution were prepared by dissolving 1.66 g of Trizma base (purity ≥99.9%, Sigma-Aldrich) and 5.72 g of Trizma hydrochloride (purity ≥99.0%, Sigma-Aldrich) into 1 litre of deionized (DI) water (Millipore Elix 5 UV, Merck Millipore, Darmstadt, Germany). The buffer solution was stored in glass bottles and kept in a fridge, and each batch was used within 4 weeks of preparation. Before use, the buffer solution was heated to 37 °C in a water bath (Julabo TW8, Julabo GmbH, Seelbach, Germany) and the pH was checked with Mettler Toledo SevenMulti pH meter using InLab Expert NTC30 probe

(resolution 0.02, Mettler-Toledo International Inc., Greifensee, Switzerland). The initial pH of all the TRIS buffer batches was 7.37±0.02 at 37.0±0.2 °C.

12 ml of TRIS buffer was pipetted at room temperature (RT) into each test tube containing the specimen and the closed tubes were placed in a shaking incubator (Infors HT Multitron, Infors AG, Bottmingen, Switzerland) set to 100 rpm and 37 °C. Test specimens were incubated for 24, 48, and 72 h and 1, 2, 4, 6, 8, and 10 weeks. To avoid saturation of the solution, the TRIS buffer in the test tubes was refreshed every two weeks.

pH of the solution was checked at 37.0±0.2 °C at the beginning of hydrolysis, with every buffer change, and at the end of the hydrolysis. TRIS buffer treated like the samples but without a specimen was used as a reference for each timepoint. After the incubation period, the samples were weighed as wet (excess water was dried with tissue paper prior to weighing), rinsed three times with DI water and left to dry. After minimum of one week in vacuum the samples were weighed again so that the water absorption and mass loss could be calculated using Equations (1) and (2):

$$Water\ absorption = \frac{wet\ mass_{final} - dry\ mass_{final}}{dry\ mass_{final}} \times 100\% \quad (1)$$

$$Mass\ loss = \frac{dry\ mass_{initial} - dry\ mass_{final}}{dry\ mass_{initial}} \times 100\% \quad (2)$$

pH, mass loss and water absorption results were calculated as averages of the parallel samples and standard deviation was used as the error.

5.3 Thermal analysis

To determine the glass content of composite samples, thermogravimetric analysis (TGA) was carried out using simultaneous thermal analyser STA 449 F1 Jupiter (NETZSCH-Gerätebau GmbH, Selb, Germany). The measurements were carried out using alumina (Al_2O_3) crucibles. The initial temperature was set at 25 °C and the end temperature at 700 °C. The used heating rate was 10 K min^{-1}. All measurements were carried out in nitrogen atmosphere, and a blank correction (two empty crucibles) was performed prior to analysis of actual samples. Sample size was 20.0±0.2 mg and for each composite, two parallel samples were analysed. The zero samples (no hydrolysis) had already been analysed when the rods were originally manufactured in the previous study [10].

Thermal analysis data was processed with NETZSCH Proteus Thermal Analysis software (version 6.1.0, NETZSCH-Gerätebau GmbH, Selb, Germany). The results of the thermal analysis were calculated as averages of the parallel measurements ± either standard deviation or minimum error of the analytical system (which ever gave the higher value).

5.4 Inductively coupled plasma optical emission spectroscopy

Ion release was monitored with inductive coupled plasma optical emission spectroscopy (ICP-OES). Samples for the ICP analysis were collected at each buffer change and at the end of the hydrolysis. The ICP samples were prepared by pipetting 5 ml of buffer solution into a 50-ml volumetric flask and filling the flask to the mark with DI water. Approximately 14 ml of this diluted solution was stored into a 15-ml plastic centrifuge tube. To prevent any microbiological growth prior to analysis, 50 µl of nitric acid (67–69%, RO-MIL-SpA super purity acid, Romil Ltd) was added to each tube. The ICP samples were stored in a fridge prior to analysis. TRIS buffer without a specimen was used as a reference for each timepoint.

The analyses were carried out using an Agilent 5110 ICP-OES (Agilent Technologies, Santa Clara, United States). The samples were analysed for potassium (K), sodium (Na), calcium (Ca), magnesium (Mg), phosphorus (P), silicon (Si), and strontium (Sr) using the wavelengths shown in Table 3 to quantify each element.

Table 3. *Wavelengths used for the ICP-OES analysis of dissolution solutions. The TRIS solutions were analysed for potassium (K), sodium (Na), calcium (Ca), magnesium (Mg), phosphorus (P), silicon (Si), and strontium (Sr).*

Element	Wavelength (nm)
K	766.491
Na	589.592
Ca	422.673
Mg	279.553
P	253.561
Si	250.690
Sr	216.596

Prior to the sample measurements, calibration curves for each element were prepared and analysed using concentration range of 4–40 ppm. Ion release results were calculated as averages of parallel measurements and standard deviation was given as the error.

5.5 Scanning electron microscopy

Scanning electron microscopy (SEM) imaging was carried out on the cross-sections of specimens immersed for 0 and 40 weeks. The aim of the imaging was to gain insight on the dissolution of the glass particles within the PLA matrix. The cross section samples were prepared by cutting approximately 1-cm piece from the 7-cm hydrolysis specimen and casting each piece into epoxy in Eppendorf tubes. The epoxy (EpoFix, Struers ApS,

Ballerup, Denmark) was prepared by mixing the resin and the hardener in 5:1 ratio. Samples were left to dry overnight and polished with Knuth-rotor 2 polishing machine (Struers, Rødovre, Denmark) using silicon carbide grinding paper up to grit 4000. Prior to analysis, all samples were coated with carbon (C) using Leica EM SCD005 cool sputter coater with CEA035 carbon evaporation accessory (Leica Microsystems GmbH, Wetzlar, Germany).

SEM imaging was performed using FEI Quanta 200F field emission gun scanning electron microscope (FEI, Hillsboro, United States) with backscatter electron detector at the Work Environment Laboratories of Finnish Institute of Occupational Health. The imaging was performed in high vacuum using 20.0 kV voltage and magnifications of 70x and 700x.

5.6 Mechanical testing

Mechanical tests for the dry samples were performed using Instron 4411 mechanical testing system (Instron Ltd., High Wycombe, United Kingdom). The 3-point bending test (Figure 8) was carried out using 500 N static load cell, 1.5 mm loading radius, 32 mm bending span, and 5 mm min^{-1} cross head speed. Shear testing (Figure 9) was carried out using the same 500 N load cell as in bending test and cross head speed of 10 mm min^{-1}.

Figure 8. *3-point bending setup used in the study. Sample diameter ca. 2 mm, sample length 7 cm, loading radius 1.5 mm, bending span 32 mm, and cross head speed 5 mm* min^{-1}.

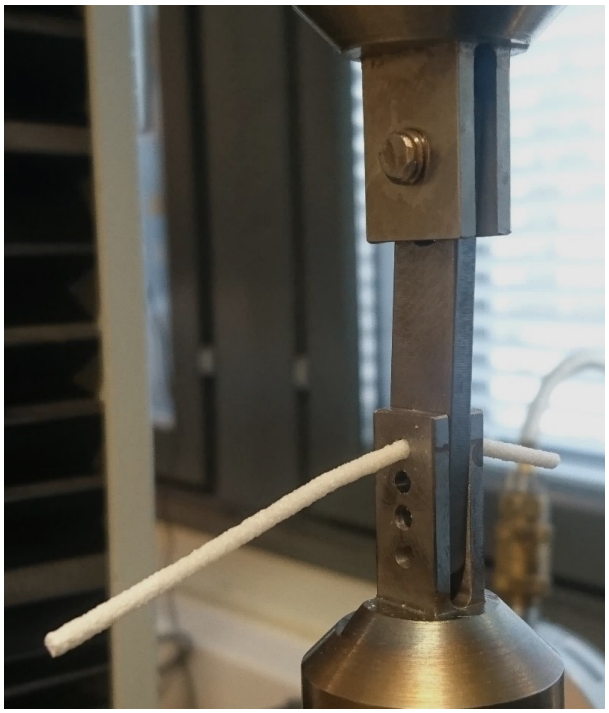

Figure 9. *Shear setup used in the study. Sample diameter is ca. 2 mm and cross head speed 10 mm* min^{-1}.

The diameter of each specimen was measured with a slide gauge (CD-15C, Mitutoyo UK Ltd, Andover, United Kingdom) from three points (both ends and the middle) and an average of these was used as the sample diameter. The mechanical tests were carried out using three parallel samples for each time point and the results have been calculated and are presented as average ± standard deviation.

6. RESULTS AND DISCUSSION

The aim of this thesis was to study the dissolution of composites manufactured using PLA as the matrix and two different types of bioactive glass as filler. The objective was to assess the effect the glass component has to the dissolution of the composite and whether the glass impacts the degradation of the polymer. Due to technical issues, the planned gel permeation chromatography (GPC) measurements had to be left out of the scope of this study, hence data from the polymer degradation is insufficient and the focus in this chapter is in the glass dissolution side of the composite *in vitro* hydrolysis.

6.1 *In vitro* hydrolysis

6.1.1 pH of the solution

During the hydrolysis study, the change in pH as a function of immersion time in TRIS was recorded. In the series where immersion time was longer than two weeks (time points 4, 6, and 8 weeks) the buffer was changed biweekly to avoid solution saturation. Each hydrolysis series had a blank TRIS control that was used to monitor changes in the pH of clean TRIS throughout the study. These changes were subtracted from the pH results of the PLA and composite samples. At each buffer change the pH returned to the baseline pH 7.37 of the TRIS. Results are given as an average of the parallel measurements and standard deviation is used as error bars in all the pH graphs. pH of the buffer solution in PLA, PLA+13-93, and PLA+Sr50 series are plotted individually in Appendix A.

Figure 10 presents the change in TRIS pH as a function of immersion time of PLA and PLA+13-93 composites.

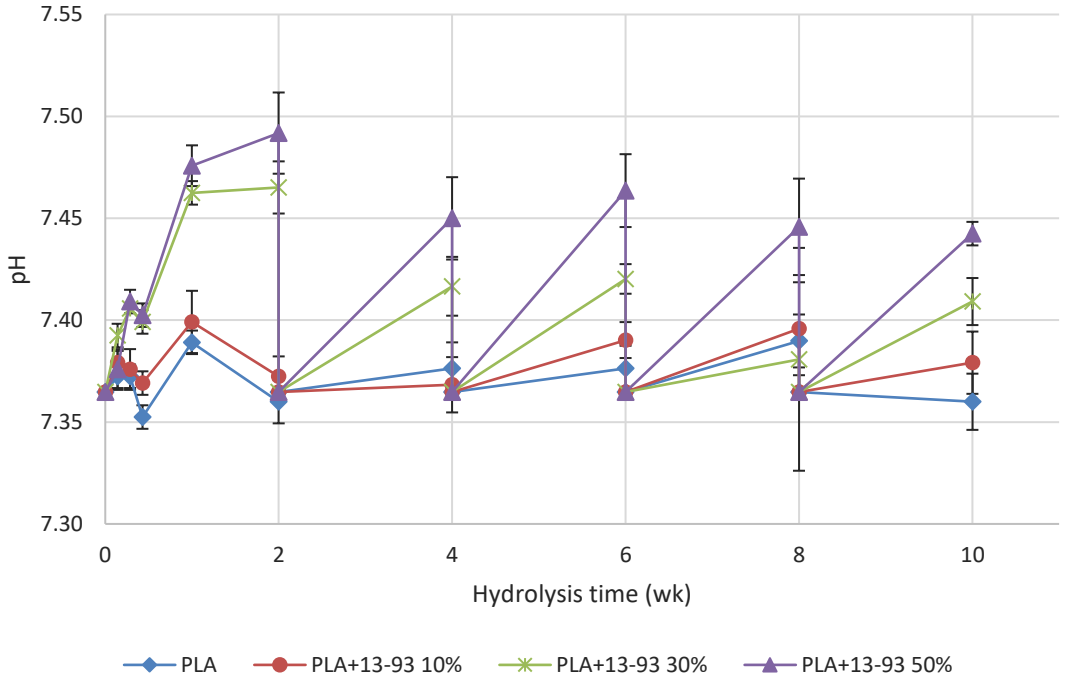

Figure 10. *pH of the TRIS solution at 37.0±0.2 °C after 24 h–10 wk of hydrolysis for pure PLA and PLA+13-93 composites. The buffer solution was refreshed every 2 weeks and at these points the pH returns to the baseline pH of 7.37.*

During hydrolysis, the pH of the solution containing pure PLA remained steady during the whole 10-week hydrolysis. PLA+13-93 composite with the lowest glass content (10%) show little pH variation compared to the pure PLA but an increase in the glass content induces a larger pH change. Increase of pH in the hydrolysis of the PLA+13-93 composites is most likely due to ion exchange and leaching of alkali and alkali earth metal ions from the composite structure to the buffer solution [45, 51–53].

Figure 11 exhibits the change in TRIS pH upon immersion of PLA and PLA+Sr50 composites.

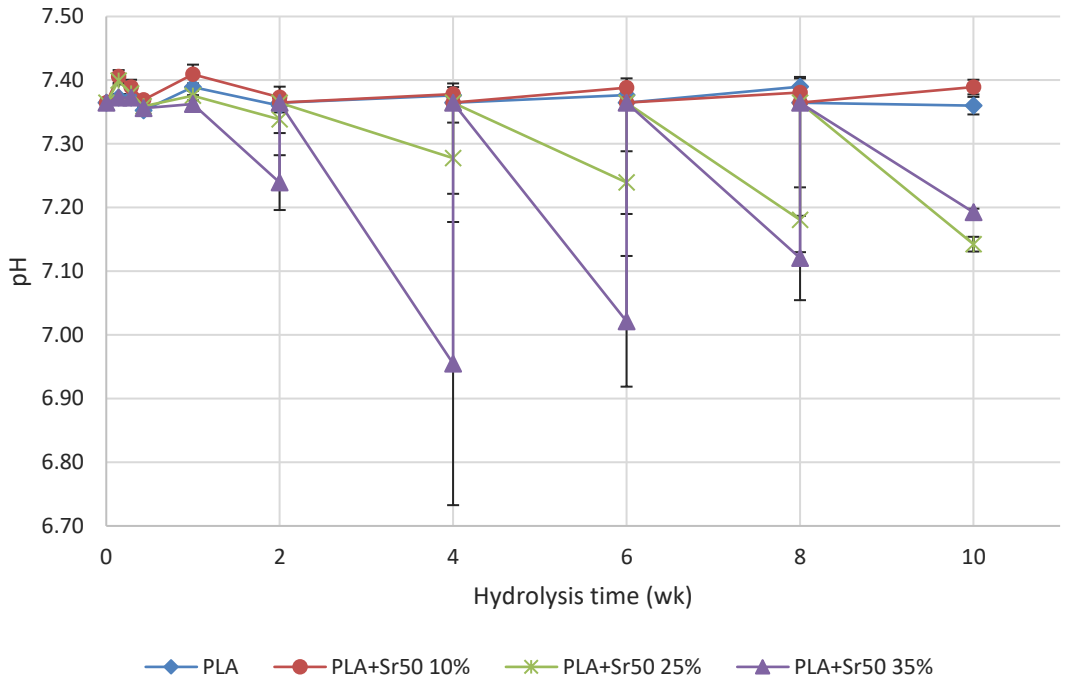

Figure 11. *pH of the TRIS solution at 37.0±0.2 °C after 24 h–10 wk of hydrolysis for pure PLA and PLA+Sr50 composites. The buffer solution was refreshed every 2 weeks and at these points the pH returns to the baseline pH of 7.37.*

As previously stated, the pH of the solution containing pure PLA remained stable over the entire 10 weeks. The pH of the solution containing composites with 10 wt% of phosphate glass also remained fairly constant over the 10-week immersion period. However, when increasing the phosphate glass concentration within the composites, a decrease in the solution pH was recorded. The higher the glass content the lower the pH for up to 8 weeks immersion. The decrease in pH of the solution containing the PLA+Sr50 composites can be explained by the release of high concentration of phosphorous which leads to the formation of phosphoric acid [29, p. 56; 54].

In both composite series, the longer the immersion time the smaller is the change in pH. This can be due to decrease in the amount and dissolution rate of the bioactive glass. The pH data obtained in this study concurs with other studies of PLA/bioactive glass composites [51, 53, 54].

6.1.2 Water absorption and mass loss

The water absorption and mass loss data presented in Figure 12–Figure 15 are averages of three parallel samples and the standard deviation has been used as the error bars. As shown in Figure 12 and Figure 13 presenting the water absorption of the pure PLA and composites containing glass 13-93 (Figure 12) and glass Sr50 (Figure 13), regardless of

the glass composition, the water uptake of the composites increases with increasing immersion time and glass content.

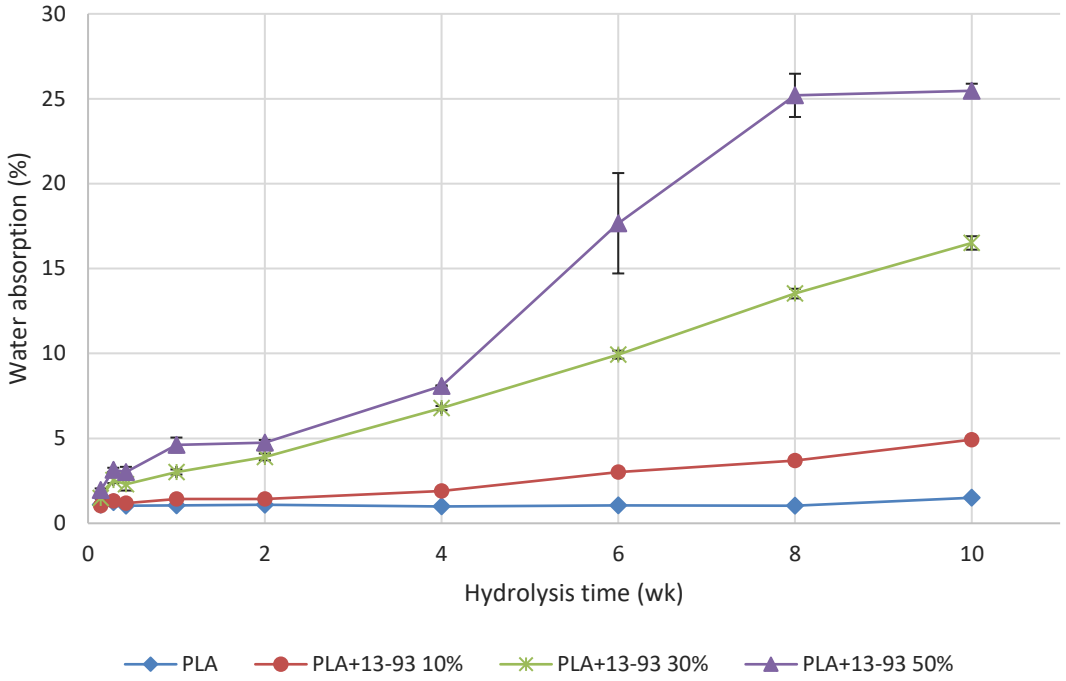

Figure 12. *Water absorption of PLA and PLA+13-93 samples after 24 h–10 wk of hydrolysis in TRIS buffer at 37 °C.*

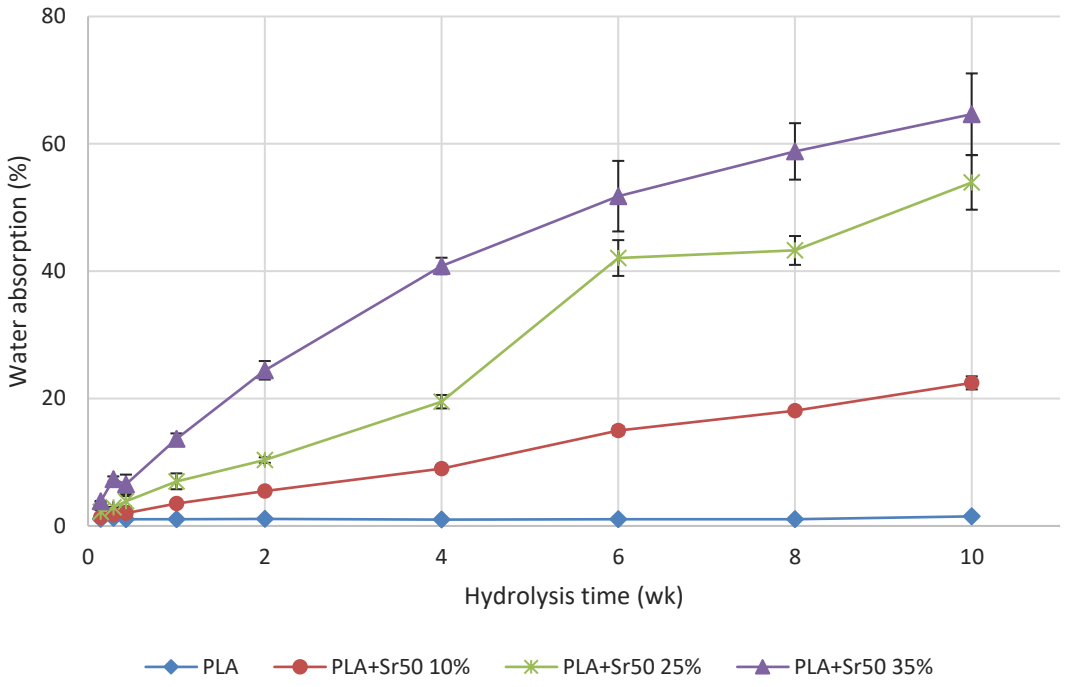

Figure 13. *Water absorption of PLA and PLA+Sr50 samples after 24 h–10 wk of hydrolysis in TRIS buffer at 37 °C.*

As expected, pure PLA shows no water absorption during 10 weeks of hydrolysis. While all six composites show some degree of water absorption during the 10-week hydrolysis, the water absorption of the PLA+Sr50 composites is much higher than that of PLA+13-93 composites. After 10 weeks of hydrolysis, the PLA+Sr50 35% composite has water absorption of 65% whereas the PLA+13-93 50% composite only has water absorption of 25%. The increased water absorption of the PLA+Sr50 composites can be related to the faster dissolution of the phosphate glass compared to the silicate glass dissolution rate [31]. These results support the hypothesis that adding bioactive glass to a polymer matrix speeds up the degradation process compared to neat polymer and the obtained results are in line with results of other studies [51, 53–56].

The water absorption results are consistent with the mass loss data shown in Figure 14 and Figure 15. When the water uptake increases, also the mass loss is increased as has been seen in other studies as well [51, 53–56].

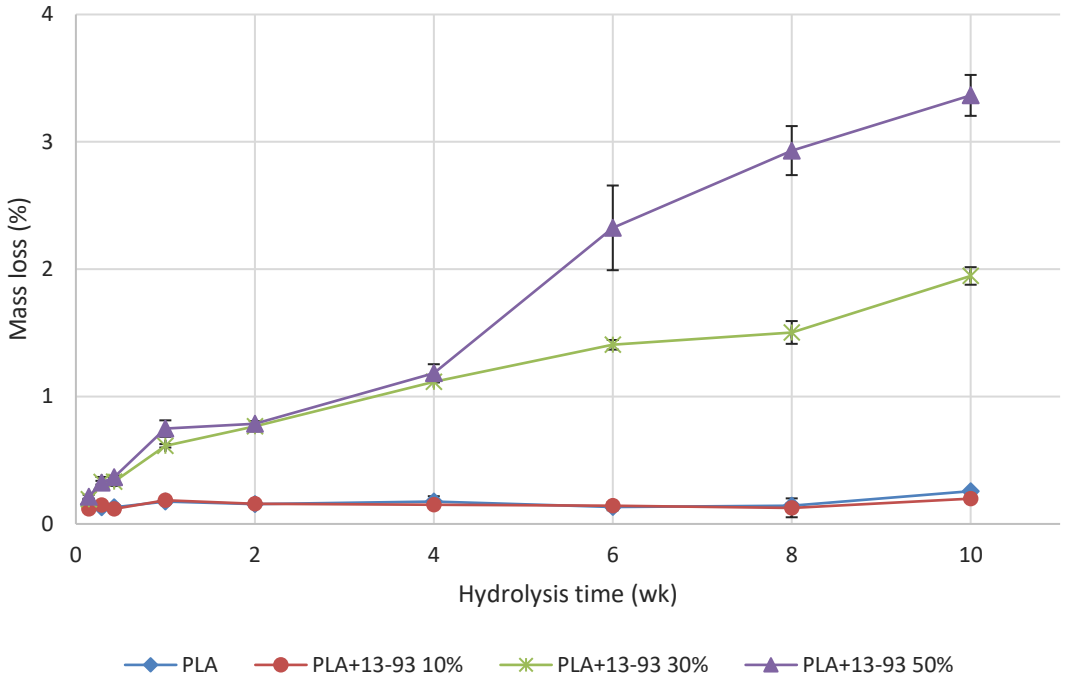

Figure 14. *Mass loss of PLA and PLA+13-93 composite samples after 24 h–10 wk of hydrolysis in TRIS buffer at 37 °C.*

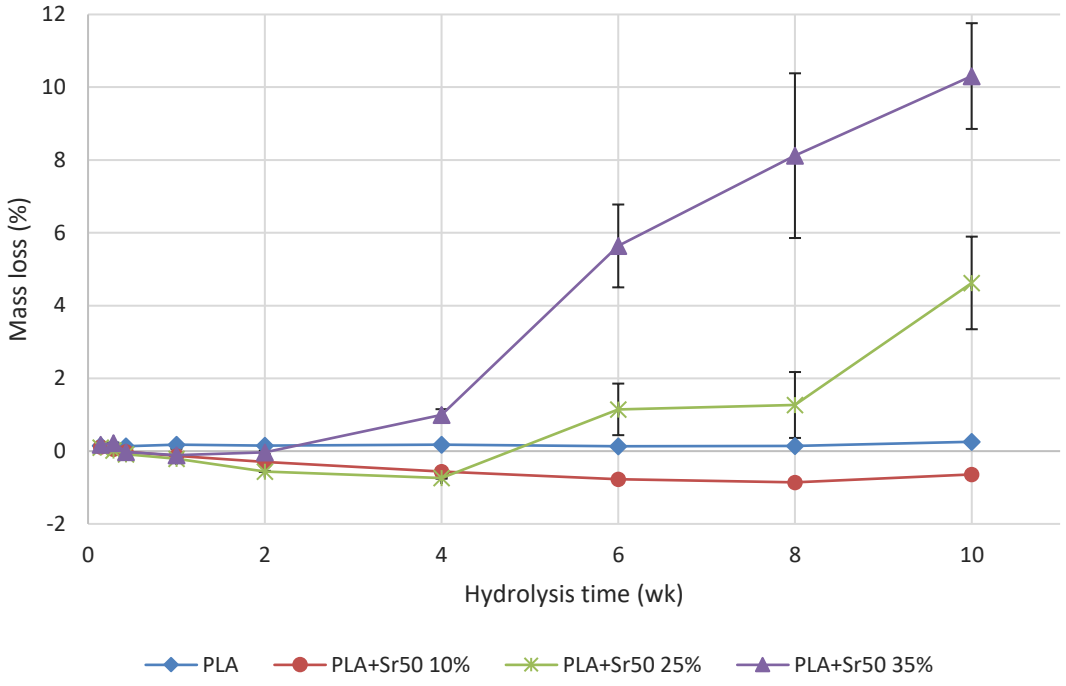

Figure 15. *Mass loss of PLA and PLA+Sr50 composite samples after 24 h–10 wk of hydrolysis in TRIS buffer at 37 °C.*

Pure PLA and composites with 10wt% of bioactive glass show no mass loss during the 10 weeks of hydrolysis. Mass loss in PLA+13-93 30/50% and PLA+Sr50 25/35% composites can be seen after four weeks of hydrolysis, mass loss increasing with increasing glass content of the composite. These results support the hypothesis that bioactive phosphate glasses undergo faster dissolution than bioactive silicate glasses. The negative mass loss of PLA and early time point samples of PLA+Sr50 25% presented in Figure 15 are likely due to insufficient drying of samples and measurement uncertainty.

6.1.3 Ion release

Figure 16–Figure 21 show the cumulative ion release of both PLA+13-93 and PLA+Sr50 composites with standard deviations of the measurements as error bars. Most of the analysed samples had concentrations below the smallest calibration concentration of 4 mg/l which caused an increase in the measurement uncertainty of the analysis. As the composites had different amounts of glass in them, the ratio of the buffer solution volume to bioactive glass mass was not constant. This must be considered when evaluating the uncertainty of the *in vitro* dissolution results.

Typically, dissolution of silicate bioactive glass, such as the 13-93, results in high initial concentrations of alkali and alkali earth metals in the solution [57]. The low sodium and potassium levels in the solution (Figure 16–Figure 18) indicate that these ions remain trapped in the polymer matrix and are not released to the solution as they would be in the case of pure silicate glass. Ion release data also show that as expected, the increase in glass content in composites result in higher amounts of ions in the buffer solution.

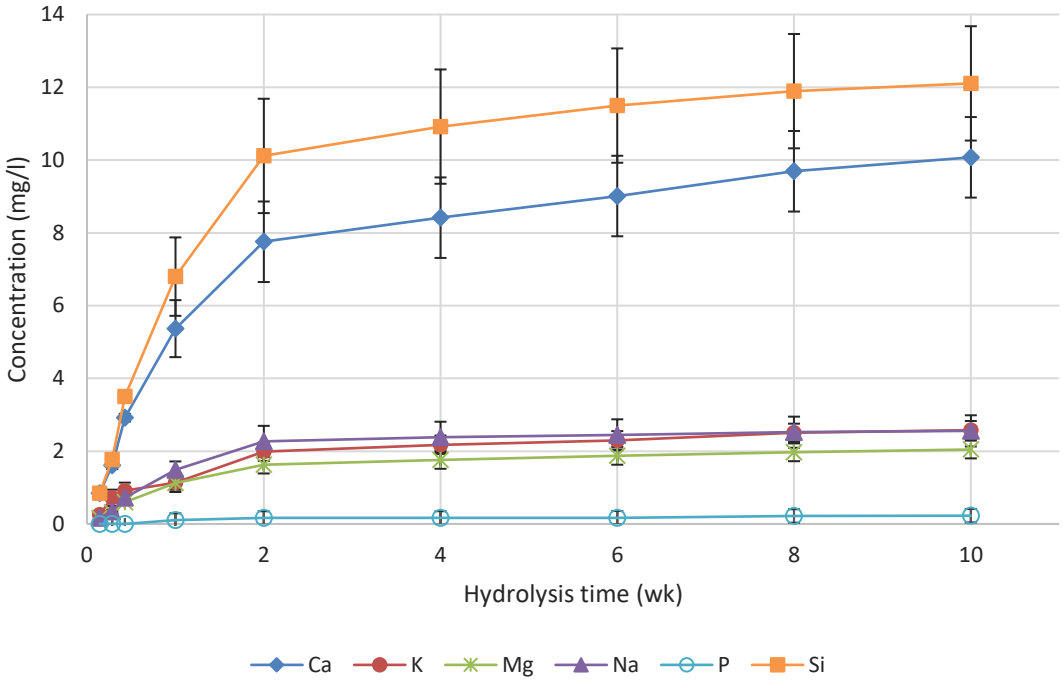

Figure 16. *Cumulative ion release of PLA+13-93 10% composite after 24 h–10 wk of hydrolysis in TRIS buffer at 37 °C.*

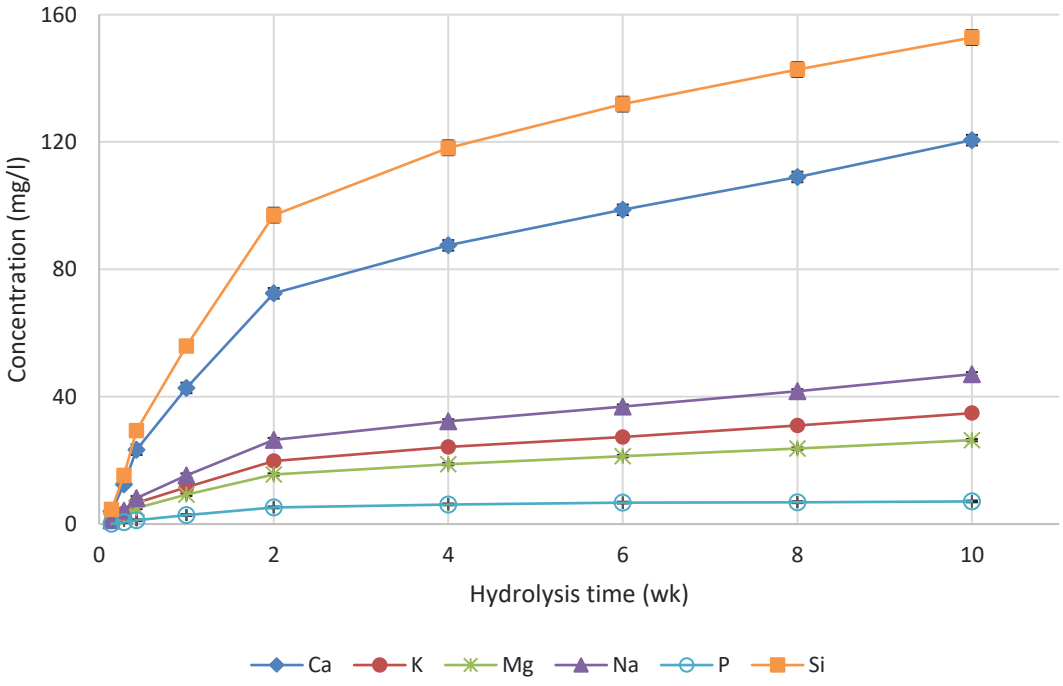

Figure 17. *Cumulative ion release of PLA+13-93 30% composite after 24 h–10 wk of hydrolysis in TRIS buffer at 37 °C.*

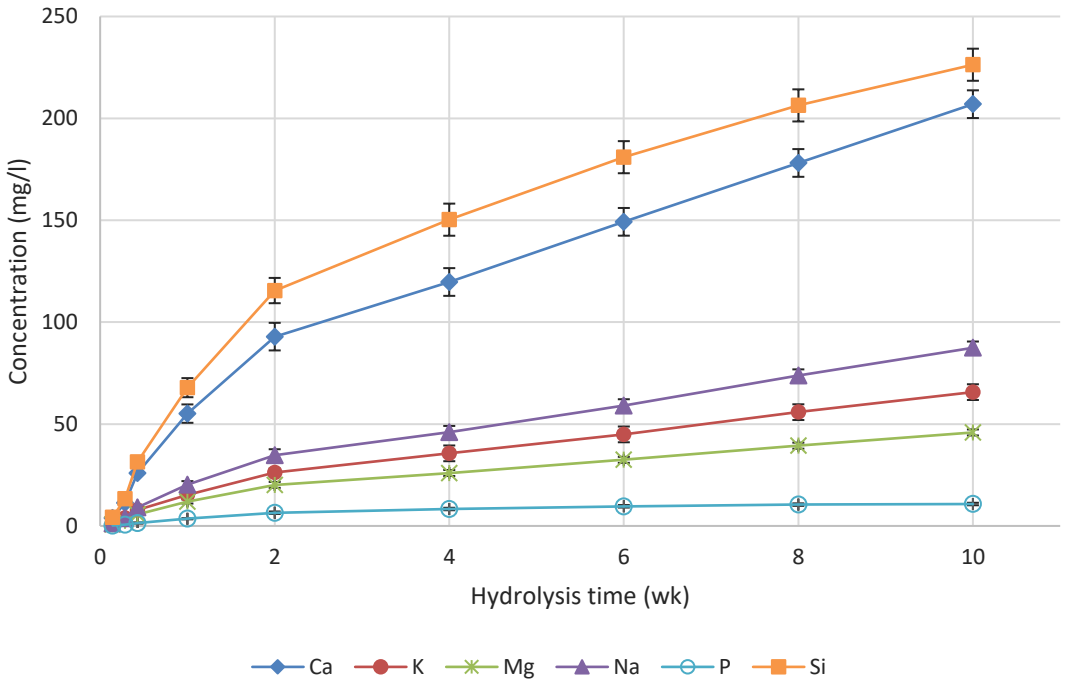

Figure 18. *Cumulative ion release of PLA+13-93 50% composite after 24 h–10 wk of hydrolysis in TRIS buffer at 37 °C.*

Ion composition in the buffer solution of the PLA+13-93 series calculated from the ICP-OES data compared to the ion composition of the original glass is presented in Table 4. These show that calcium is over-represented in the buffer solution while sodium and potassium are present in concentrations similar to those in the glass. These results were unanticipated, as the expectation was that both Na and K would leach out of the composite in the early stages and the cumulative release of these species would plateau. A study by Houaoui *et al.* [58] got similar results using PLA+13-93 composites.

Table 4. *Ion composition of the modified bioactive glass 13-93 and the TRIS solution after 1, 2, and 10 weeks of hydrolysis of PLA+13-93 composites at 37 °C. Compositions are given as molecular percentages (mol%).*

Composite glass content (%)	Hydrolysis time (wk)	SiO_2 (mol%)	P_2O_5 (mol%)	CaO (mol%)	Na_2O (mol%)	MgO (mol%)	K_2O (mol%)
Pure 13-93	-	55	2	22	8	8	6
10	1	51	0.4	28	7	10	3
	2	52	0.4	28	7	10	4
	10	50	0.4	29	6	10	4
30	1	50	1	27	8	10	4
	2	51	1	27	8	9	4
	10	49	1	27	9	10	4
50	1	49	1	28	9	10	4
	2	49	1	27	9	10	4
	10	45	1	29	11	10	5

Phosphate glass dissolution occurs by dissolution of the phosphate chains resulting in the same ion composition in the solution as the initial glass composition [29, 31]. Whereas in the PLA+13-93 composites the glass is affected by polymer retention, in the PLA+Sr50 composites the phosphate chains are released in controlled fashion resulting in higher ion concentrations in the buffer solution (Figure 19–Figure 21) and faster dissolution. As with the PLA+13-93 series, also PLA+Sr50 composites show an increase in ion concentrations of the buffer solution when the glass content in the composites increase.

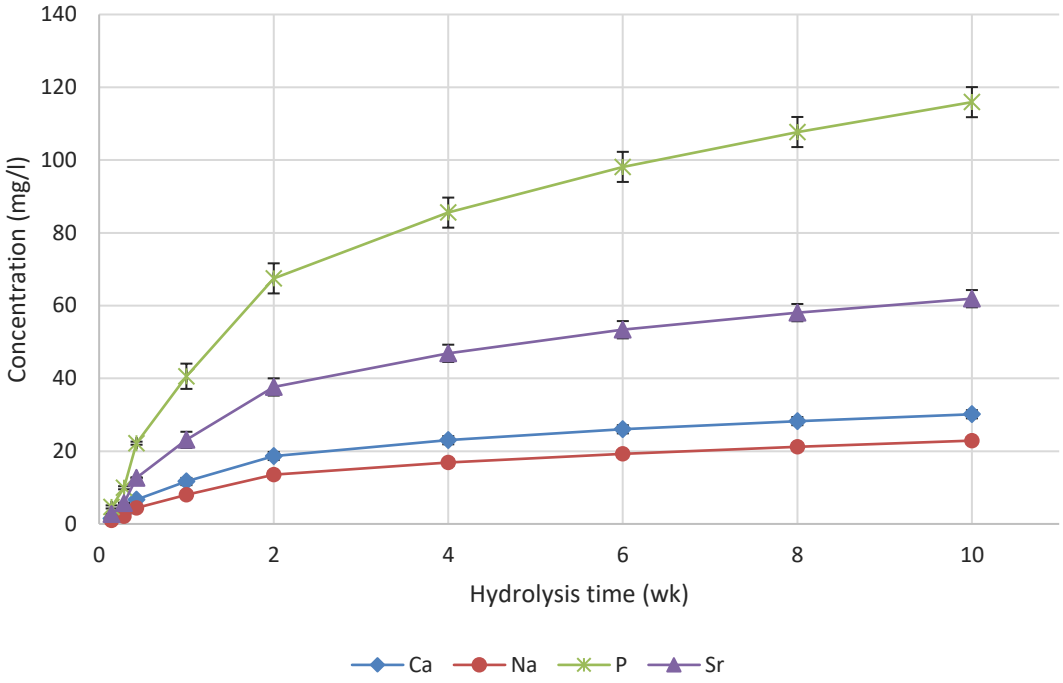

Figure 19. *Cumulative ion release of PLA+Sr50 10% composite after 24 h–10 wk hydrolysis in TRIS buffer at 37 °C.*

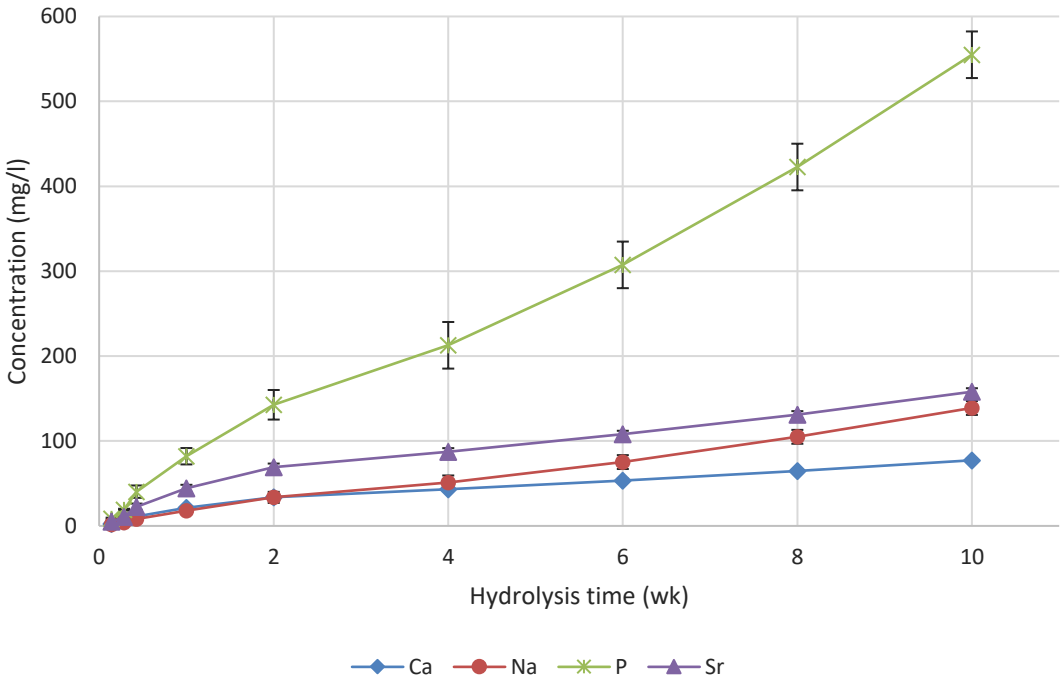

Figure 20. *Cumulative ion release of PLA+Sr50 25% composite after 24 h–10 wk of hydrolysis in TRIS buffer at 37 °C.*

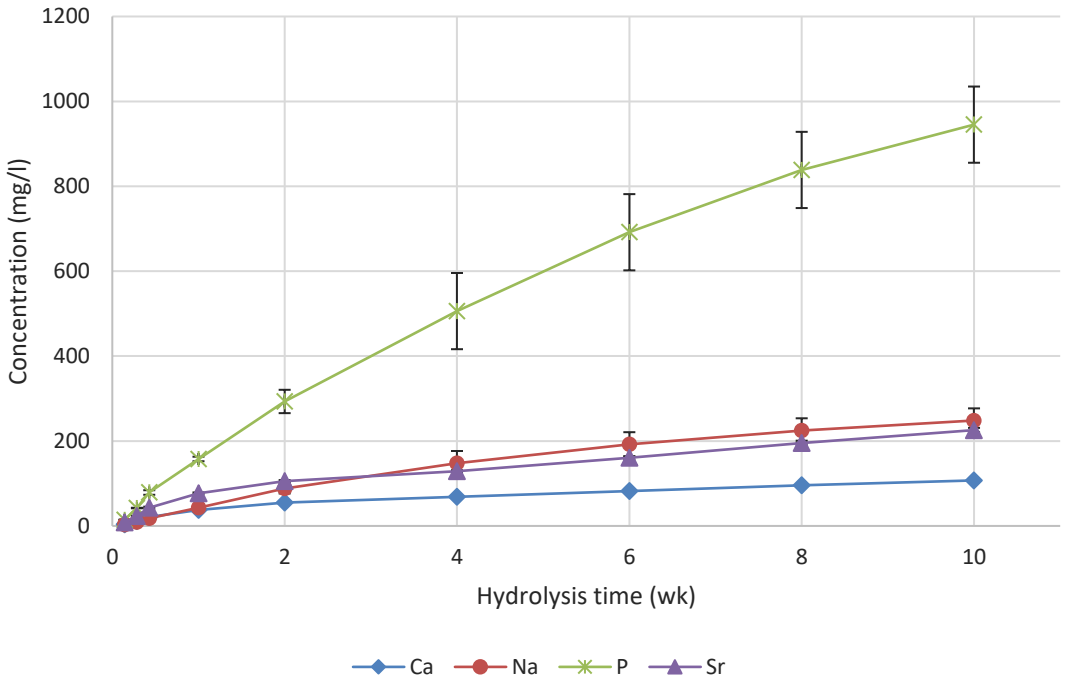

Figure 21. *Cumulative ion release of PLA+Sr50 35% composite after 24 h–10 wk of hydrolysis in TRIS buffer at 37 °C.*

Ion composition in the buffer solution of the PLA+Sr50 series calculated from the ICP-OES data compared to the ion composition of the original glass is presented in Table 5.

Table 5. *Ion composition of the bioactive glass Sr50 and the TRIS solution after 1, 2, and 10 weeks of hydrolysis of PLA+Sr50 composites at 37 °C. Compositions are given as molecular percentages (mol%).*

Composite glass content (%)	Hydrolysis time (wk)	P_2O_5 (mol%)	CaO (mol%)	Na_2O (mol%)	SrO (mol%)
Pure Sr50	-	50	20	10	20
10	1	47	21	13	19
	2	48	20	13	19
	10	49	20	13	18
25	1	48	19	14	18
	2	49	18	16	17
	10	57	12	19	11
35	1	48	18	18	17
	2	51	15	21	13
	10	59	10	21	10

The data in Table 5 show that phosphate glass dissolution indeed results into the same ion composition in the buffer solution as the original glass – at least in the beginning. After 10 weeks of hydrolysis in composites with higher glass content (25/35%) both Ca and Sr concentration in the solution is only approximately 50% of the amount of these elements in the original glass. This is most likely due to precipitation of calcium- and strontium phosphate as demonstrated in studies by Mishra *et al.* [59, 60] and Massera *et al.*[61].

6.2 Structural properties

After 10 weeks of hydrolysis only the PLA, PLA+13-93 10% and PLA+Sr50 10% samples exhibited noticeable changes in their appearance. As shown in Figure 22, during the hydrolysis both 10% composites had turned from sort of crystalline appearance (Figure 7) to white, while the pure PLA had turned from clear to white only in one end of the test specimen.

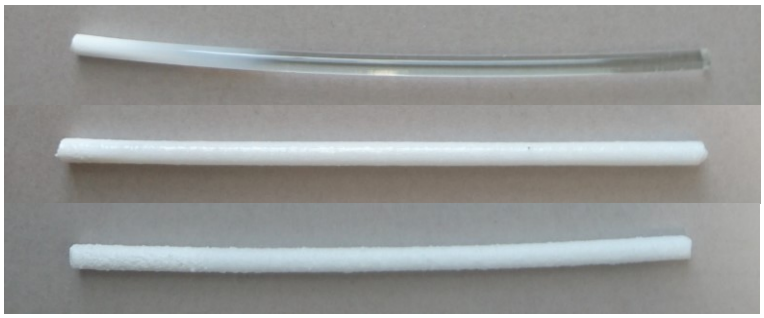

Figure 22. *Test specimens after 10 weeks of hydrolysis in TRIS buffer at 37 °C. From top: PLA, PLA+13-93 10% and PLA+Sr50 10%.*

From the selected few 40-week hydrolysis samples of the previous study [10] imaged with SEM (see 6.2.2), the PLA+13-93 50% composite rods had swollen and the samples were extremely brittle. Meanwhile the PLA+Sr50 35% composite rods remained relatively similar in appearance compared to before the hydrolysis.

6.2.1 Thermogravimetric analysis

The results of TGA measurements presented in Table 6 are given as an average of the two parallel measurements with difference of maximum value and average as the error. The TGA plots are presented in Appendix B.

Table 6. *Average residual masses as percentage by weight (wt%) of the composite samples using thermogravimetric analysis after 0, 4, 10, and 40 weeks (wk) of hydrolysis in TRIS at 37 °C.*

Hydrolysis time (wk)	Average residual mass (wt%)					
	PLA+13-93			PLA+Sr50		
	10%	30%	50%	10%	25%	35%
0	9 ± 2	32 ± 1	48 ± 3	11 ± 1	25 ± 3	34 ± 1
4	8 ± 1	33 ± 1	40 ± 1	9 ± 1	19 ± 1	24 ± 1
10	12 ± 1	30 ± 1	44 ± 1	10 ± 1	19 ± 1	23 ± 1
40	12 ± 1	25 ± 1	41 ± 1	6 ± 1	10 ± 1	15 ± 1

Composites with 10% of bioactive glass show little change in the glass content even after 40 weeks of hydrolysis. Substantial drop in the amount of inorganic parts within the composites are recorded for samples with medium to high glass content. The glass mass content decrease from (32 ± 1)% to (25 ± 1)% and (48 ± 3)% to (41 ± 1)% for the PLA+13-93 30 and 50% composites. The decrease in the mass content is even more drastic for the composites containing the phosphate glass. The mass content of glass decreases from (25 ± 3)% to (10 ± 1)% and (34 ± 1)% to (15 ± 1)% for the PLA+Sr50 25 and 35% composite samples. The lower remnant glass in the case of the PLA+Sr50 composites is in agreement with the faster dissolution rate of the phosphate glass compared to the silicate glass.

As TGA cannot separate glass from other inorganic solids, it is possible that the measured values are not 100% glass but contain for instance some CaP that has formed during the hydrolysis.

6.2.2 Scanning electron microscopy

The SEM images of composite samples that have not been in hydrolysis (Figure 23) show that the PLA+Sr50 composite rods manufactured in the previous study [10] had uneven glass distribution. Also, the particle size range is wider than the 125–250 μm originally reported for both composite types. The higher particle size distribution is most likely due to breakage of the particles during processing. The uneven distribution of glass within the PLA+Sr50 composite is likely caused by the higher density of the phosphate glass which could have caused the glass to accumulate on one side of the composite rod during extrusion.

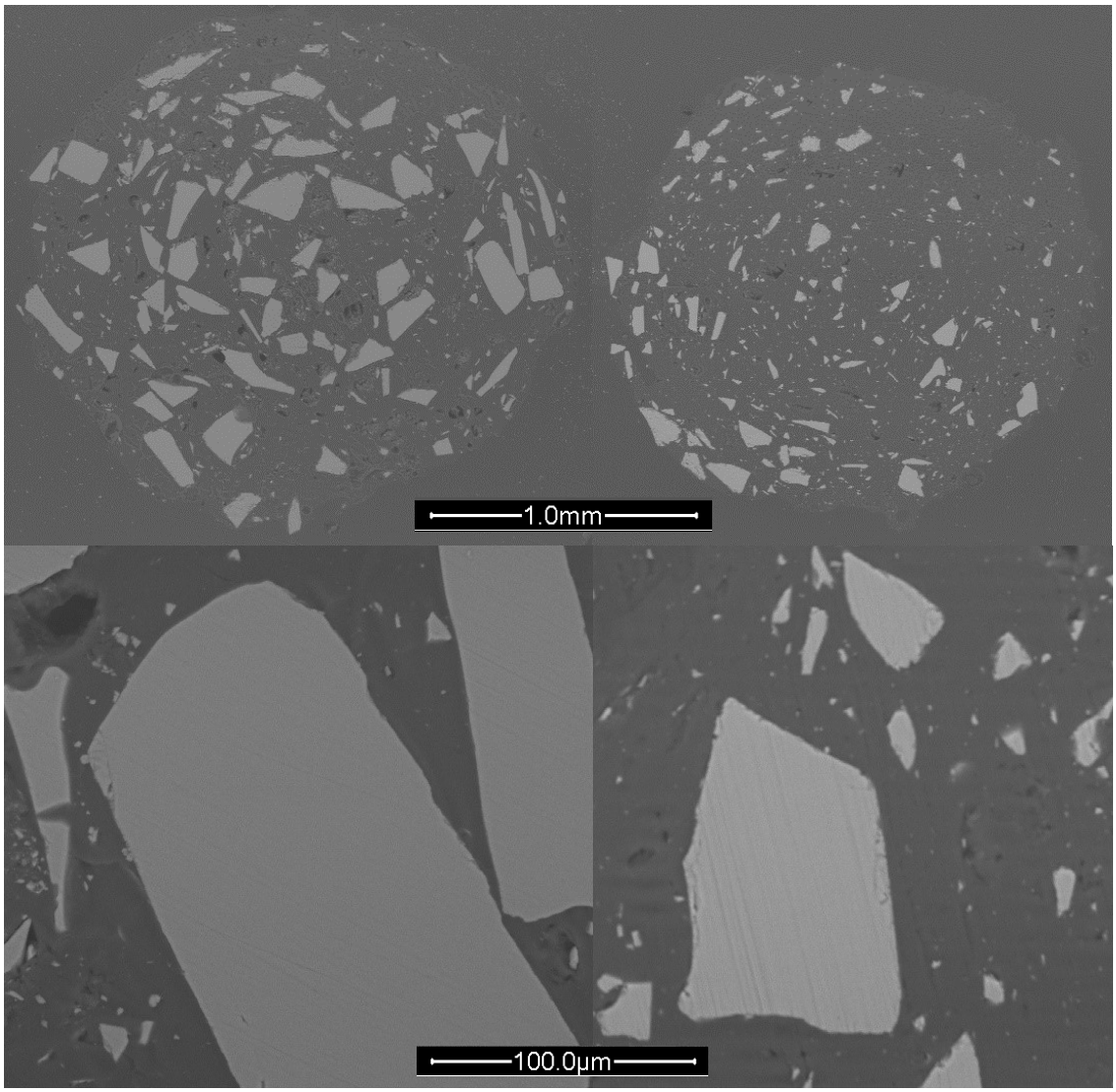

Figure 23. *Backscatter electron SEM images of composite rod cross sections of 0-week PLA+13-93 50% (on left) and PLA+Sr50 35% (on right). In the images glass particles are shown as white and PLA shows as transparent. Magnification used in the top two images is 70x and in the lower two images 700x.*

The SEM images of the composites with the highest glass content (Figure 24) show that after 40 weeks of hydrolysis the silicate glass composite had more glass particles left in it than the phosphate glass composite. Additionally, the structure of the silicate composite seems to be more porous than the phosphate composite. After 40 weeks of hydrolysis, the phosphate composite has almost no glass left.

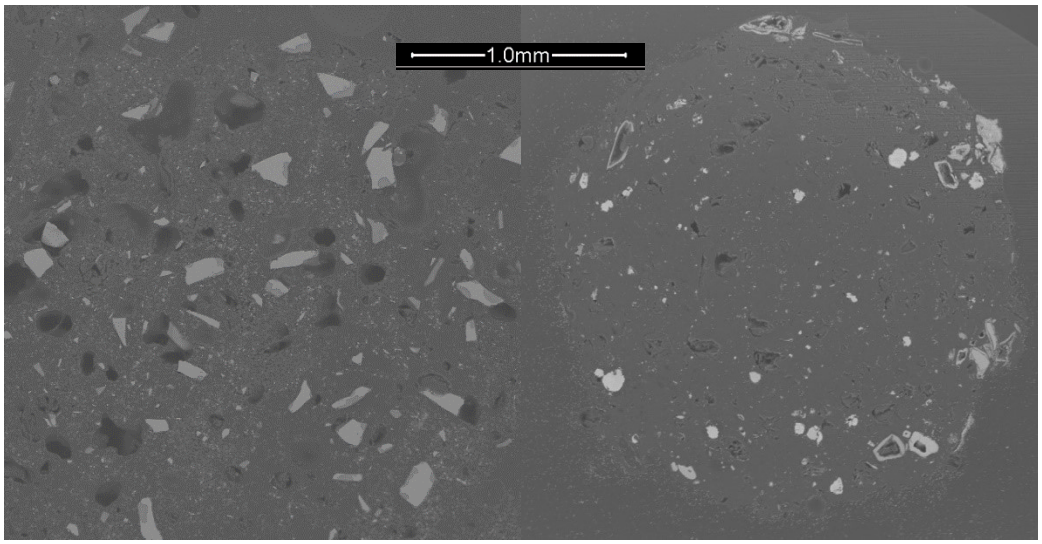

Figure 24. *Backscatter electron SEM images of composite rod cross sections of 40-week PLA+13-93 50% (on left) and PLA+Sr50 35% (on right). In the images glass particles are shown as white and PLA shows as transparent. Magnification used in the images is 70x. The full cross section of the PLA+13-93 50% rod does not fit in the image as the rod had swollen significantly during hydrolysis.*

The SEM imaging of the test specimens support the ion release data and the conclusion that the phosphate glass dissolves more rapidly than the silicate glass.

6.3 Mechanical properties

Addition of bioactive glass to the PLA matrix decreases the stress at maximum load in both bending and shear tests (Figure 25–Figure 28). The graphs show the average of parallel measurements and standard deviation has been used as error bars.

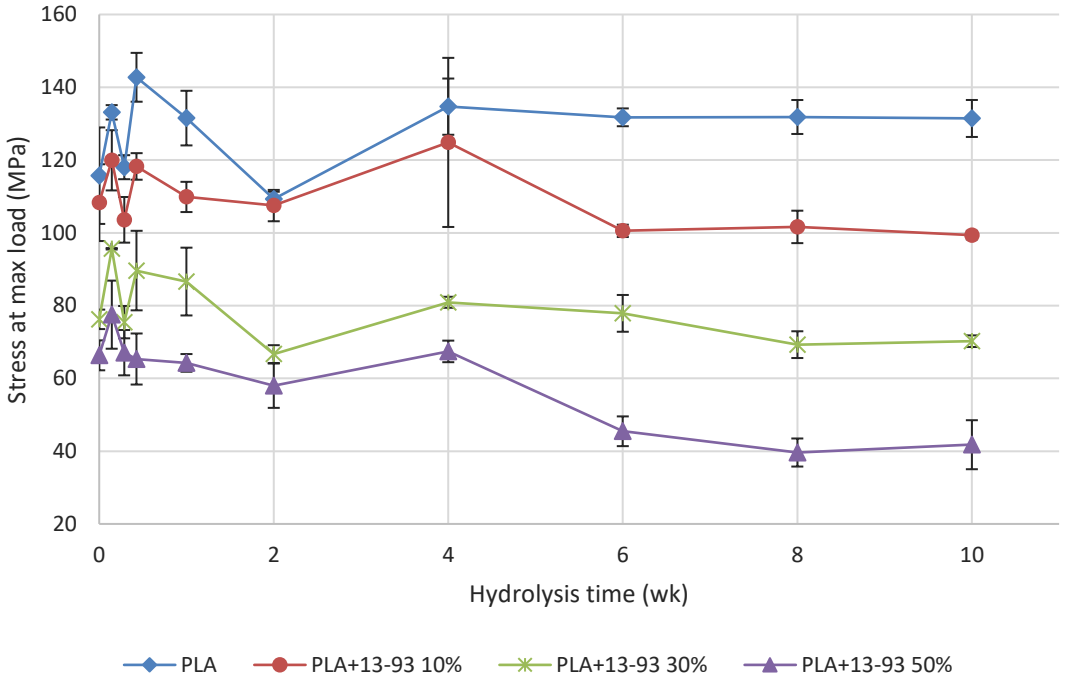

Figure 25. *The three-point bending test results of dried PLA and PLA+13-93 composites after 0–10 wk of hydrolysis in TRIS at 37 °C.*

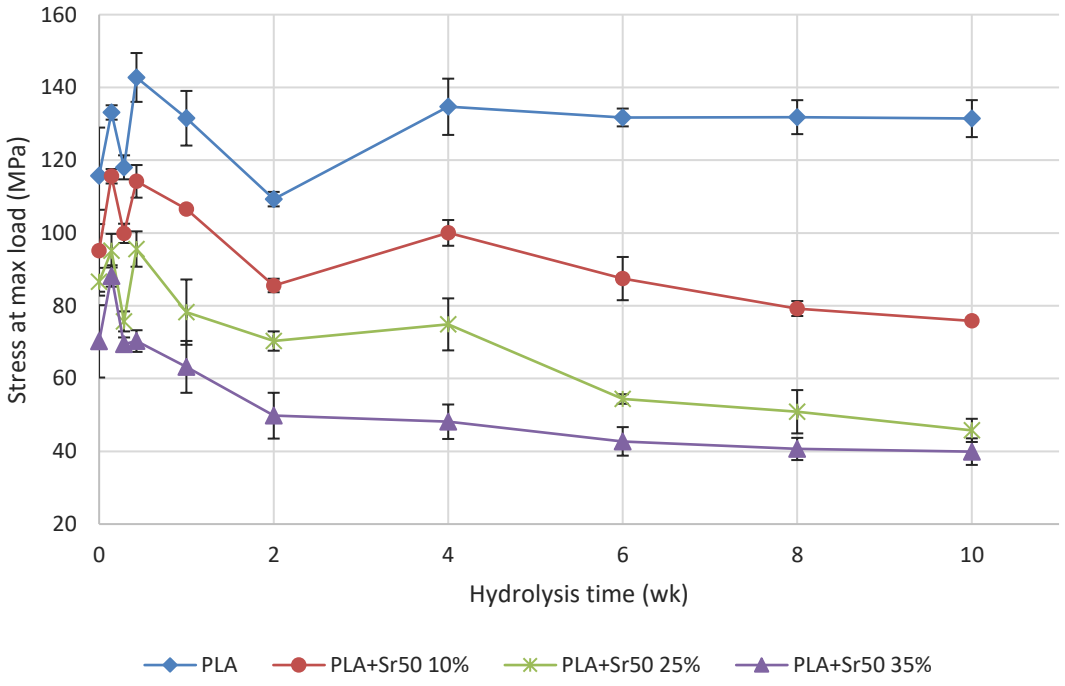

Figure 26. *The three-point bending test results of dried PLA and PLA+Sr50 composites after 0–10 wk of hydrolysis in TRIS at 37 °C.*

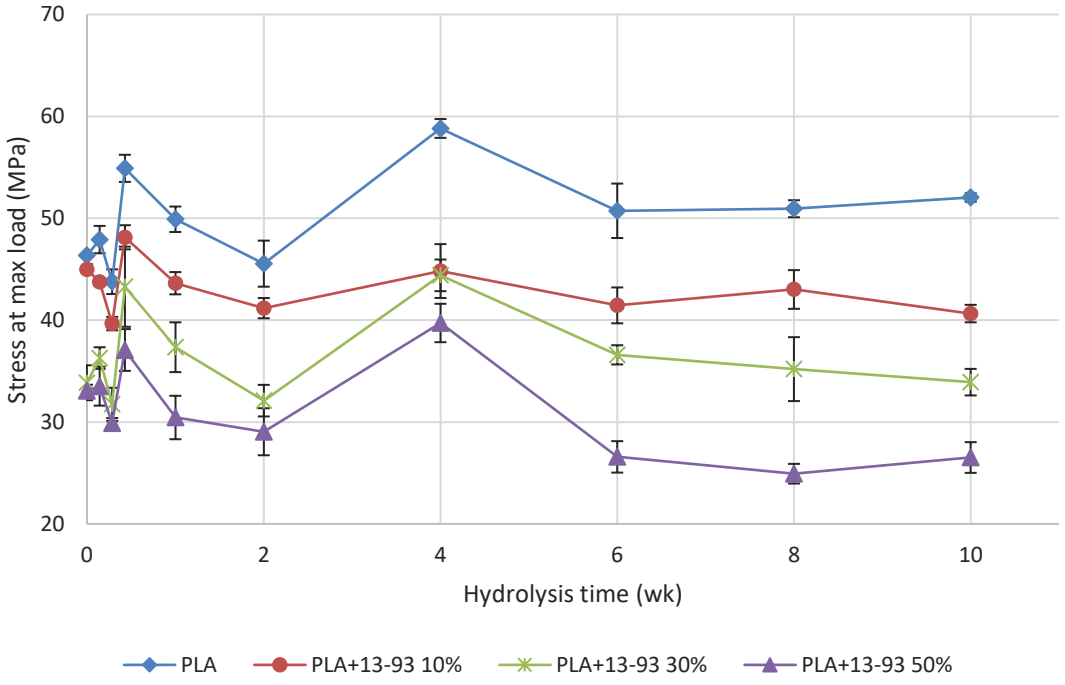

Figure 27. *The shear test results of dried PLA and PLA+13-93 composites after 0–10 wk of hydrolysis in TRIS at 37 °C.*

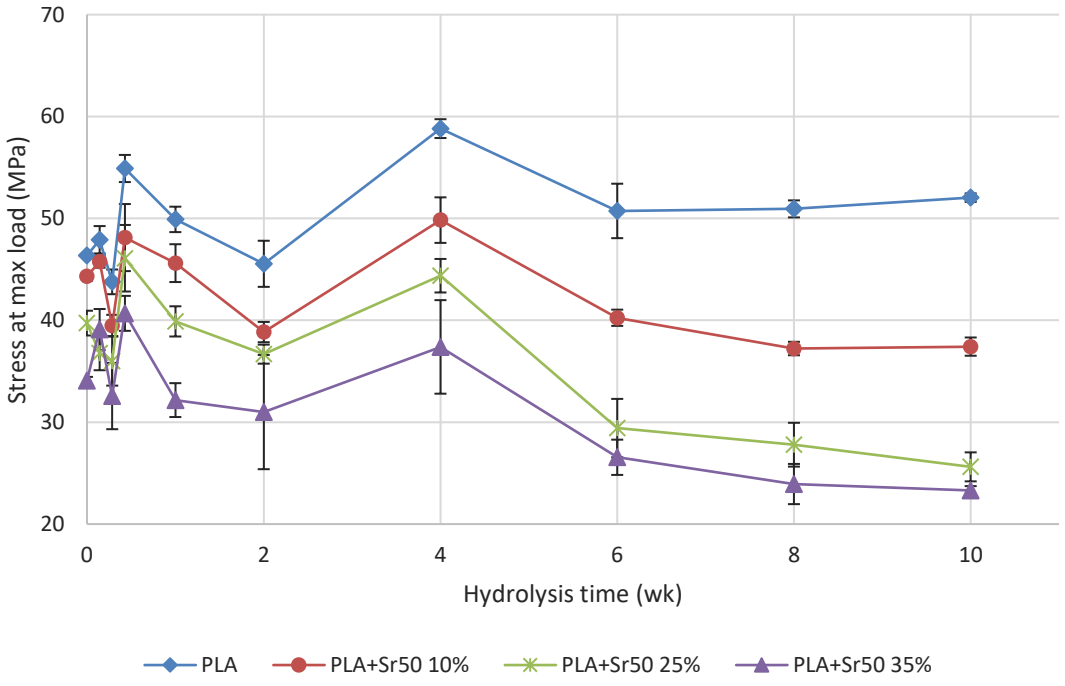

Figure 28. *The shear test results of dried PLA and PLA+Sr50 composites after 0–10 wk of hydrolysis in TRIS at 37 °C.*

The change in the initial mechanical properties is a function of the glass content but independent of glass composition. The PLA rods did not show changes in mechanical properties up to 10 weeks of hydrolysis. In fact, only PLA+13-93 50% and the PLA+Sr50 composites show a noticeable decrease of mechanical properties in the bending test after 10 weeks of hydrolysis: -37% (PLA+13-93 50%), -20% (PLA+Sr50 10%), -47% (PLA+Sr50 25%), and -43% (PLA+Sr50 35%). Other studies have also reported that addition of bioactive glass to a polymer matrix decreases the mechanical properties compared to neat polymer [53]. No publications using composites manufactured in the same way as in this study was found, so no direct comparison can be made.

In the case of the PLA+13-93 composite, the decrease in mechanical properties with immersion time, is likely due to the increase in porosity. For the PLA+Sr50 composites, the decrease in mechanical properties can be assigned to the large dissolution of particles leaving voids within the polymer matrix.

7. CONCLUSIONS

The aim of this thesis was to investigate how bioactive glasses release ions through polymer matrix in composite structure and how different bioactive glasses react with the polymer matrix, thus changing the properties of the composite. The dissolution of PLA and six PLA/bioactive glass composites were studied during 10 weeks of *in vitro* hydrolysis in TRIS buffer at 37 °C. The composite rods had different amounts of either modified silicate glass 13-93 or phosphate glass Sr50. During the hydrolysis pH, mass loss, water absorption, ion release, glass content, and mechanical properties were studied.

During 10 weeks of hydrolysis, no substantial changes in pH, mass or mechanical properties of the pure PLA could be observed. Composites with the lowest glass content (10%) showed little difference compared with the pure PLA, however an increase in the glass content induces changes in solution pH, sample mass and water uptake. It was shown that the glass particles dissolve through the polymer matrix. As expected, the phosphate glass dissolved faster than the silicate glass and composites degraded faster than pure PLA. Enhanced degradation rate of the composites was manifested by higher weight loss and decrease in mechanical properties. The results also indicate that the higher the glass content in the composite, the more the mechanical properties of the composite decrease and the faster the glass dissolves.

Based on both SEM imaging and visual observations, the composite rods used in the study were not as homogeneous as they could have. Thus, the results may have higher uncertainty. However, as a conclusion based on the results of this study, the degradation of PLA/bioactive glass composites is greatly dependent on the type of glass used as filler and the amount of glass used. As the amount and distribution of glass in extruded composites seem to have higher than desired variation, research on other methods of manufacturing such composites is called for. As technical problems prevented the GPC analysis, this data needs to be obtained to verify the effects of glass addition to the polymer matrix.

REFERENCES

[1] L.L. Hench, O. Andersson, Bioactive Glasses, in: L.L. Hench (ed.), An Introduction to Bioceramics, 2nd ed., Imperial College Press, London, United Kingdom, 2013, pp. 49–69.

[2] L.L. Hench, J. Wilson, Introduction, in: L.L. Hench (ed.), An Introduction to Bioceramics, 2nd ed., Imperial College Press, London, United Kingdom, 2013, pp. 1–26.

[3] L. Hench, The story of Bioglass, Journal of Materials Science: Materials in Medicine, Vol. 17, Iss. 11, 2006, pp. 967–978.

[4] L.L. Hench, Bioceramics: From Concept to Clinic, Journal of the American Ceramic Society, Vol. 74, Iss. 7, 1991, pp. 1487–1510.

[5] D.C. Greenspan, Bioactive glass: mechanisms of bone bonding, Tandläkartidningen, Vol. 91, Iss. 8, 1999.

[6] D.S. Brauer, Bioactive Glasses—Structure and Properties, Angewandte Chemie International Edition, Vol. 54, Iss. 14, 2015, pp. 4160–4181.

[7] J.C. Middleton, A.J. Tipton, Synthetic biodegradable polymers as orthopedic devices, Biomaterials, Vol. 21, Iss. 23, 2000, pp. 2335–2346.

[8] K. Rezwan, Q.Z. Chen, J.J. Blaker, A.R. Boccaccini, Biodegradable and bioactive porous polymer/inorganic composite scaffolds for bone tissue engineering, Biomaterials, Vol. 27, Iss. 18, 2006, pp. 3413–3431.

[9] R.K. Kulkarni, K.C. Pani, C. Neuman, F. Leonard, Polylactic Acid for Surgical Implants, Archives of Surgery, Vol. 93, Iss. 5, 1966, pp. 839-843.

[10] S. Ghimire, *In vitro* and mechanical properties of bioactive glass/polymer composites, Master's thesis, Tampere University of Technology, Department of Electronics and Communications Engineering, Tampere, 2016, 59 p. Available: http://URN.fi/URN:NBN:fi:tty-201606174271.

[11] X. Qi, Y. Ren, X. Wang, New advances in the biodegradation of Poly(lactic) acid, International Biodeterioration & Biodegradation, Vol. 117, 2017, pp. 215–223.

[12] R. Auras, B. Harte, S. Selke, An overview of polylactides as packaging materials, Macromolecular Bioscience, Vol. 4, Iss. 9, 2004, pp. 835–864.

[13] D. Garlotta, A Literature Review of Poly(Lactic Acid), Journal of Polymers and the Environment, Vol. 9, Iss. 2, 2001, pp. 63–84.

[14] J.R. Fried, Polymer science and technology, 2nd ed. Prentice Hall Professional Technical Reference, Upper Saddle River, New Jersey, United States, 2003, 582 p.

[15] L.T. Sin, A.R. Rahmat, Rahman, W A W A, Polylactic Acid: PLA Biopolymer Technology and Applications, William Andrew, Kidligton, United Kingdom, 2012, 341 p.

[16] H.R. Allcock, F.W. Lampe, J.E. Mark, Contemporary Polymer Chemistry, 3rd ed. Pearson Education, Inc., Upper Saddle River, United States, 2003, 814 p.

[17] A.P. Gupta, V. Kumar, New emerging trends in synthetic biodegradable polymers – Polylactide: A critique, European Polymer Journal, Vol. 43, Iss. 10, 2007, pp. 4053–4074.

[18] M.P. Stevens, Polymer chemistry: an introduction, 2nd ed. Oxford University Press, Inc., New York, United States, 1990, 633 p.

[19] Polymers: A Property Database, Poly(lactide), CRC Press, web page. Available (accessed 16.7.2017): http://poly.chemnetbase.com.

[20] K. Madhavan Nampoothiri, N.R. Nair, R.P. John, An overview of the recent developments in polylactide (PLA) research, Bioresource Technology, Vol. 101, Iss. 22, 2010, pp. 8493–8501.

[21] A. Södergård, M. Stolt, Properties of lactic acid based polymers and their correlation with composition, Progress in Polymer Science, Vol. 27, Iss. 6, 2002, pp. 1123–1163.

[22] J.P. Penning, H. Dijkstra, A.J. Pennings, Preparation and properties of absorbable fibres from l-lactide copolymers, Polymer, Vol. 34, Iss. 5, 1993, pp. 942–951.

[23] L.S. Nair, C.T. Laurencin, Biodegradable polymers as biomaterials, Progress in Polymer Science, Vol. 32, Iss. 8–9, 2007, pp. 762–798.

[24] J. Lunt, Large-scale production, properties and commercial applications of polylactic acid polymers, Polymer Degradation and Stability, Vol. 59, Iss. 1–3, 1998, pp. 145–152.

[25] J. Clayden, N. Greeves, S. Warren, Organic chemistry, 2nd ed. Oxford University Press, Oxford, United Kingdom, 2012, 1234 p.

[26] F. von Burkersroda, L. Schedl, A. Göpferich, Why degradable polymers undergo surface erosion or bulk erosion, Biomaterials, Vol. 23, Iss. 21, 2002, pp. 4221–4231.

[27] L.L. Lao, N.A. Peppas, F.Y.C. Boey, S.S. Venkatraman, Modeling of drug release from bulk-degrading polymers, International Journal of Pharmaceutics, Vol. 418, Iss. 1, 2011, pp. 28–41.

[28] L.L. Hench, J.W. Hench, D.C. Greenspan, Bioglass: A Short History and Bibliography, Journal of the Australasian Ceramic Society, Vol. 40, Iss. 1, 2004, pp. 1–42.

[29] D.S. Brauer, Phosphate Glasses, in: J.R. Jones, A.G. Clare (ed.), Bio-glasses: an introduction, John Wiley & Sons Ltd, Chichester, United Kingdom, 2012, pp. 45–64.

[30] W.D. Callister, D.G. Rethwisch, Materials Science and Engineering, 8th SI version ed. John Wiley & Sons, Inc., Hoboken, New Jersey, United States, 2011, 885 p.

[31] B.C. Bunker, G.W. Arnold, J.A. Wilder, Phosphate glass dissolution in aqueous solutions, Journal of Non-Crystalline Solids, Vol. 64, Iss. 3, 1984, pp. 291–316.

[32] A.N. Cormack, The Structure of Bioactive Glasses and Their Surfaces, in: J.R. Jones, A.G. Clare (ed.), Bio-glasses: an introduction, John Wiley & Sons Ltd, Chichester, United Kingdom, 2012, pp. 65–74.

[33] T. Kokubo, Apatite formation on surfaces of ceramics, metals and polymers in body environment, Acta Materialia, Vol. 46, Iss. 7, 1998, pp. 2519–2527.

[34] J.C. Knowles, Phosphate based glasses for biomedical applications, Journal of Materials Chemistry, Vol. 13, Iss. 10, 2003, pp. 2395–2401.

[35] E.A. Abou Neel, D.M. Pickup, S.P. Valappil, R.J. Newport, J.C. Knowles, Bioactive functional materials: a perspective on phosphate-based glasses, Journal of Materials Chemistry, Vol. 19, 2009, pp. 690–701.

[36] L.L. Hench, D.E. Clark, Physical chemistry of glass surfaces, Journal of Non-Crystalline Solids, Vol. 28, Iss. 1, 1978, pp. 83–105.

[37] R.W. Douglas, T.M.M. El-Shamy, Reactions of Glasses with Aqueous Solutions, Journal of the American Ceramic Society, Vol. 50, Iss. 1, 1967, pp. 1–8.

[38] W. Liang, C. Rüssel, D.E. Day, G. Völksch, Bioactive comparison of a borate, phosphate and silicate glass, Journal of Materials Research, Vol. 21, Iss. 1, 2006, pp. 125–131.

[39] F. Delahaye, L. Montagne, G. Palavit, J.C. Touray, P. Baillif, Acid dissolution of sodium–calcium metaphosphate glasses, Journal of Non-Crystalline Solids, Vol. 242, Iss. 1, 1998, pp. 25–32.

[40] M. Dziadek, E. Stodolak-Zych, K. Cholewa-Kowalska, Biodegradable ceramic-polymer composites for biomedical applications: A review, Materials Science and Engineering: C, Vol. 71, 2017, pp. 1175–1191.

[41] A. Kelly, A. Mortensen, Composite Materials: Overview, in: K.H.J. Buschow, R.W. Cahn, M.C. Flemings, B. Ilschner, E.J. Kramer, S. Mahajan, P. Veyssière (ed.), Encyclopedia of Materials: Science and Technology, 2nd ed., Elsevier Science Ltd, Oxford, United Kingdom, 2001, pp. 1361–1371.

[42] M.F. Ashby, Composite Materials, Microstructural Design of, in: K.H.J. Buschow, R.W. Cahn, M.C. Flemings, B. Ilschner, E.J. Kramer, S. Mahajan, P. Veyssière (ed.), Encyclopedia of Materials: Science and Technology, 2nd ed., Elsevier Science Ltd, Oxford, United Kingdom, 2001, pp. 1357–1361.

[43] K.K. Chawla, Composite materials: Science and Engineering, 3rd ed. Springer, New York, 2012, 542 p.

[44] I.M. Daniel, O. Ishai, Engineering Mechanics of Composite Materials, 2nd ed. Oxford University Press, New York, United States, 2006, 396 p.

[45] A.R. Boccaccini, V. Maquet, Bioresorbable and bioactive polymer/Bioglass® composites with tailored pore structure for tissue engineering applications, Composites Science and Technology, Vol. 63, Iss. 16, 2003, pp. 2417–2429.

[46] A.R. Boccaccini, J.A. Roether, L.L. Hench, V. Maquet, R. Jéròme, A composites approach to tissue engineering, Ceramic Engineering and Science Proceedings, pp. 805–816.

[47] Q. Fu, E. Saiz, M.N. Rahaman, A.P. Tomsia, Bioactive glass scaffolds for bone tissue engineering: state of the art and future perspectives, Materials Science & Engineering C, Vol. 31, Iss. 7, 2011, pp. 1245–1256.

[48] E. Pamula, J. Kokoszka, K. Cholewa-Kowalska, M. Laczka, L. Kantor, L. Niedzwiedzki, G. Reilly, J. Filipowska, W. Madej, M. Kolodziejczyk, G. Tylko, A. Osyczka, Degradation, Bioactivity, and Osteogenic Potential of Composites Made of PLGA and Two Different Sol–Gel Bioactive Glasses, Annals of Biomedical Engineering; The Journal of the Biomedical Engineering Society, Vol. 39, Iss. 8, 2011, pp. 2114–2129.

[49] J.R. Jones, Review of bioactive glass: From Hench to hybrids, Acta Biomaterialia, Vol. 9, Iss. 1, 2013, pp. 4457–4486.

[50] J. Rich, T. Jaakkola, T. Tirri, T. Närhi, A. Yli-Urpo, J. Seppälä, In vitro evaluation of poly(ε-caprolactone-co-DL-lactide)/bioactive glass composites, Biomaterials, Vol. 23, Iss. 10, 2002, pp. 2143–2150.

[51] V. Maquet, A.R. Boccaccini, L. Pravata, I. Notingher, R. Jérôme, Preparation, characterization, and in vitro degradation of bioresorbable and bioactive composites based on Bioglass®-filled polylactide foams, Journal of Biomedical Materials Research Part A, Vol. 66A, Iss. 2, 2003, pp. 335–346.

[52] H. Li, J. Chang, pH-compensation effect of bioactive inorganic fillers on the degradation of PLGA, Composites Science and Technology, Vol. 65, Iss. 14, 2005, pp. 2226–2232.

[53] H. Niiranen, T. Pyhältö, P. Rokkanen, M. Kellomäki, P. Törmälä, In vitro and in vivo behavior of self-reinforced bioabsorbable polymer and self-reinforced bioabsorbable polymer/bioactive glass composites, Journal of Biomedical Materials Research Part A, Vol. 69A, Iss. 4, 2004, pp. 699–708.

[54] G. Georgiou, L. Mathieu, D.P. Pioletti, P.- Bourban, J.-E. Månson, J.C. Knowles, S.N. Nazhat, Polylactic acid–phosphate glass composite foams as scaffolds for bone tissue engineering, Journal of Biomedical Materials Research Part B: Applied Biomaterials, Vol. 80B, Iss. 2, 2007, pp. 322–331.

[55] G. Vergnol, N. Ginsac, P. Rivory, S. Meille, J. Chenal, S. Balvay, J. Chevalier, D.J. Hartmann, *In vitro* and *in vivo* evaluation of a polylactic acid-bioactive glass composite for bone fixation devices, Journal of Biomedical Materials Research Part B, Vol. 104, Iss. 1, 2016, pp. 180–191.

[56] T. Niemelä, H. Niiranen, M. Kellomäki, Self-reinforced composites of bioabsorbable polymer and bioactive glass with different bioactive glass contents. Part II: In vitro degradation, Acta Biomaterialia, Vol. 4, Iss. 1, 2008, pp. 156–164.

[57] M.D. O'Donnell, Melt-Derived Bioactive Glass, in: J.R. Jones, A.G. Clare (ed.), Bio-glasses: an introduction, John Wiley & Sons Ltd, Chichester, United Kingdom, 2012, pp. 13–27.

[58] A. Houaoui, I. Lyyra, R. Agniel, E. Pauthe, J. Massera, M. Boissière, Dissolution, bioactivity and osteogenic properties of composites based on polymer and silicate or borosilicate bioactive glass, Materials Science and Engineering: C, Vol. 107, 2020, article 110340.

[59] A. Mishra, J. Rocherullé, J. Massera, Ag-doped phosphate bioactive glasses: thermal, structural and *in-vitro* dissolution properties, Biomedical Glasses, Vol. 2, Iss. 1, 2016, pp. 38–48.

[60] A. Mishra, L. Petit, M. Pihl, M. Andersson, T. Salminen, J. Rocherullé, J. Massera, Thermal, structural and in vitro dissolution of antimicrobial copper-doped and slow resorbable iron-doped phosphate glasses, Journal of Materials Science, Vol. 52, Iss. 15, 2017, pp. 8957–8972.

[61] J. Massera, L. Petit, T. Cardinal, J.J. Videau, M. Hupa, L. Hupa, Thermal properties and surface reactivity in simulated body fluid of new strontium ion-containing phosphate glasses, Journal of Materials Science: Materials in Medicine, Vol. 24, Iss. 6, 2013, pp. 1407–1416.

APPENDIX A: pH DATA OF INDIVIDUAL SAMPLE TYPES

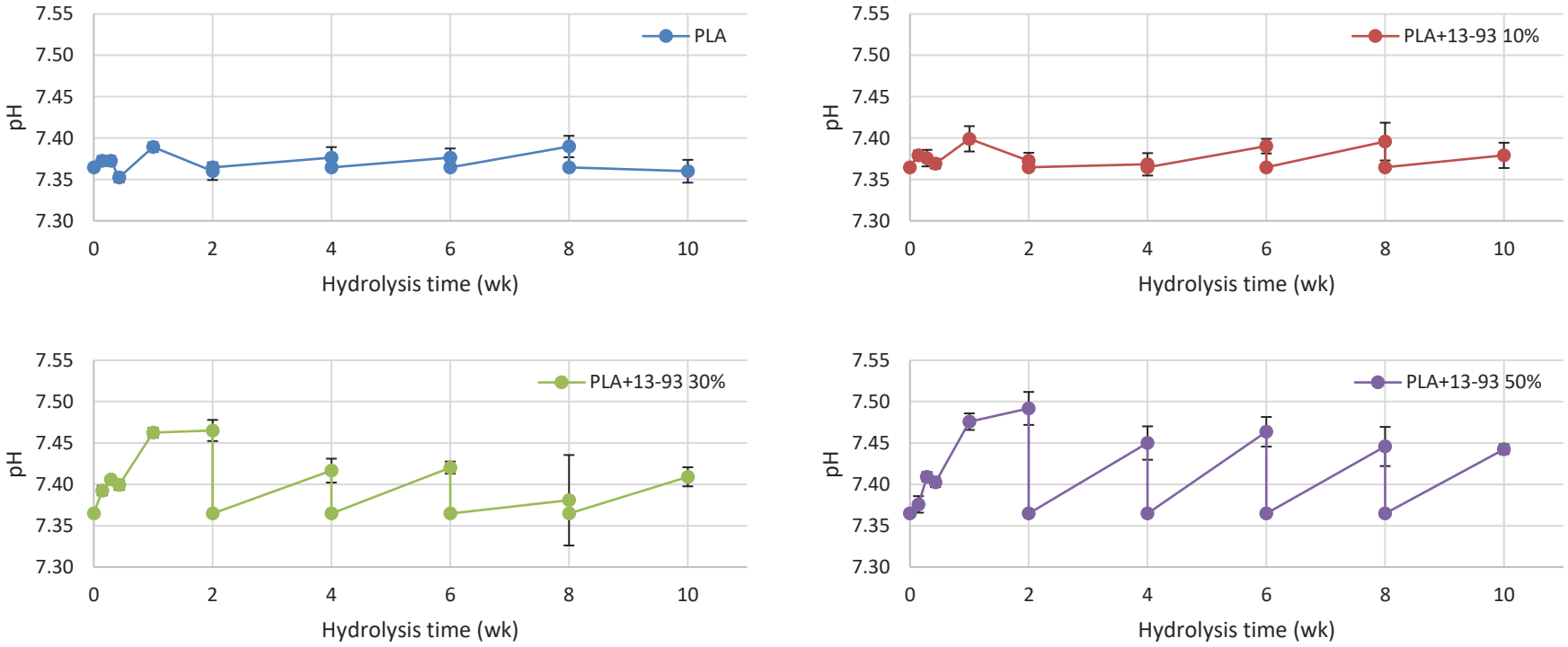

Figure A-1. *pH of the TRIS buffer solution at 37.0±0.2 °C after 24 h–10 wk of hydrolysis for pure PLA and PLA+13-93 composites. The buffer solution was changed every 2 weeks and at these points the pH returns to the baseline pH of 7.37.*

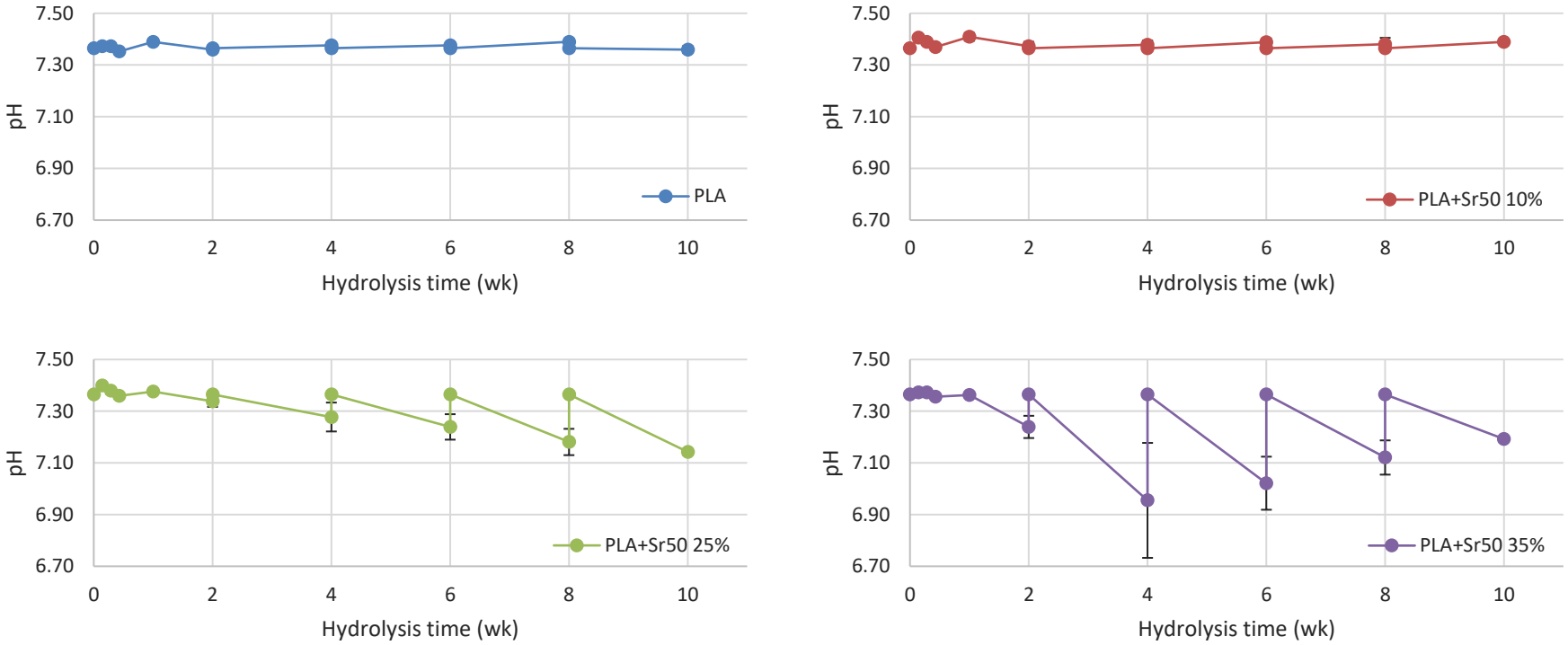

Figure A-2. *pH of the TRIS buffer solution at 37.0±0.2 °C after 24 h–10 wk of hydrolysis for pure PLA and PLA+Sr50 composites. The buffer solution was changed every 2 weeks and at these points the pH returns to the baseline pH of 7.37.*

APPENDIX B: TGA GRAPHS

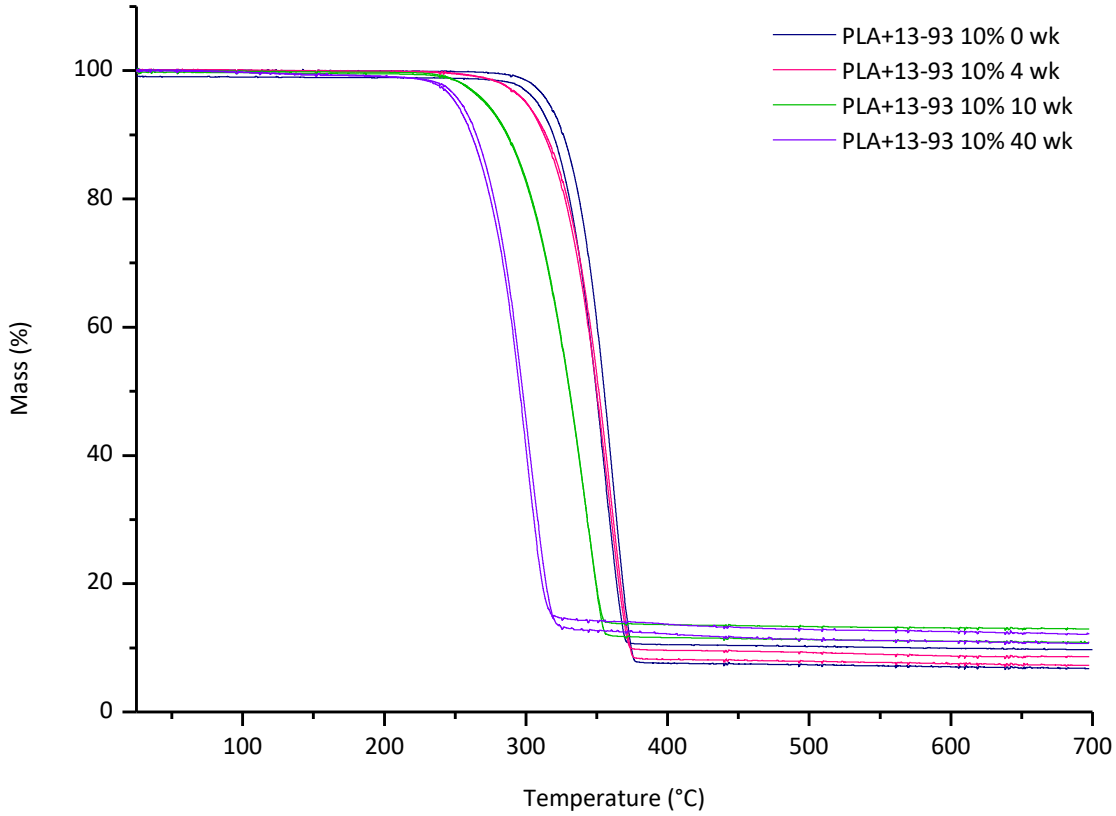

Figure B-1. *TGA graphs of PLA+13-93 10% composite after 0, 4, 10, and 40 weeks of hydrolysis in TRIS at 37 °C. For each time point, two parallel measurements were done.*

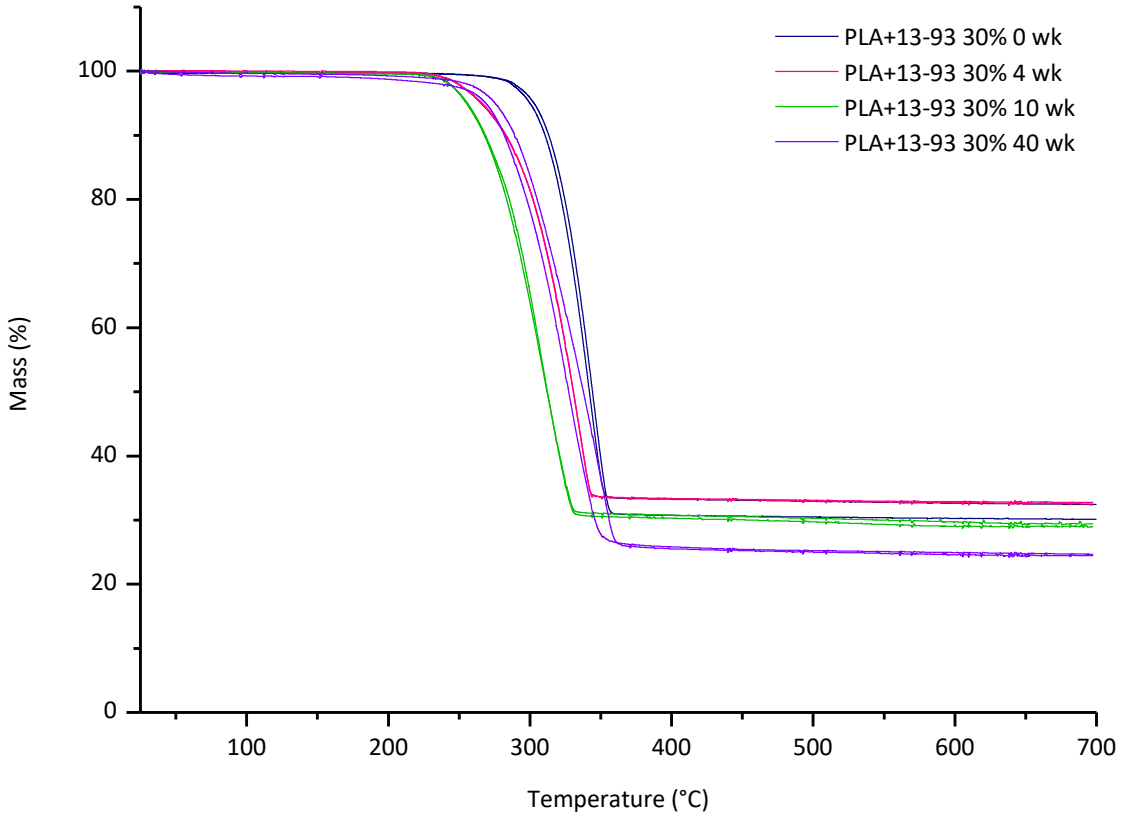

Figure B-2. *TGA graphs of PLA+13-93 30% composite after 0, 4, 10, and 40 weeks of hydrolysis in TRIS at 37 °C. For each time point, two parallel measurements were done.*

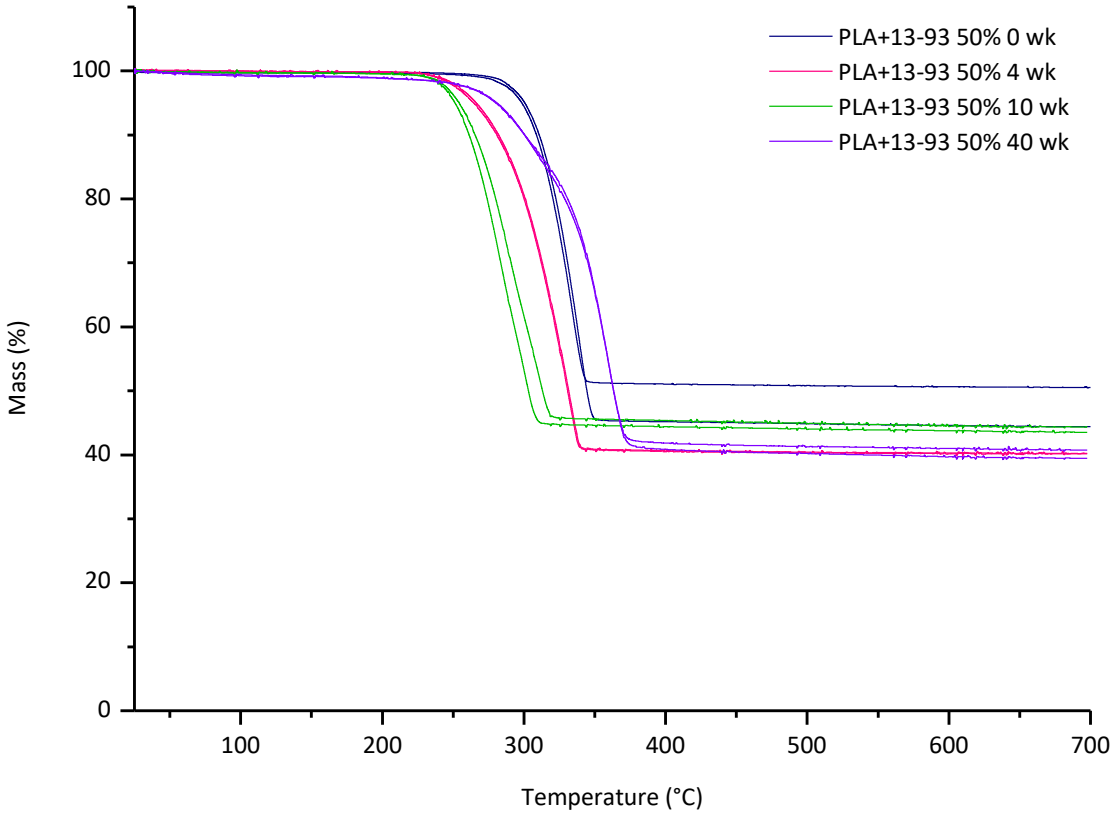

Figure B-3. *TGA graphs of PLA+13-93 50% composite after 0, 4, 10, and 40 weeks of hydrolysis in TRIS at 37 °C. For each time point, two parallel measurements were done.*

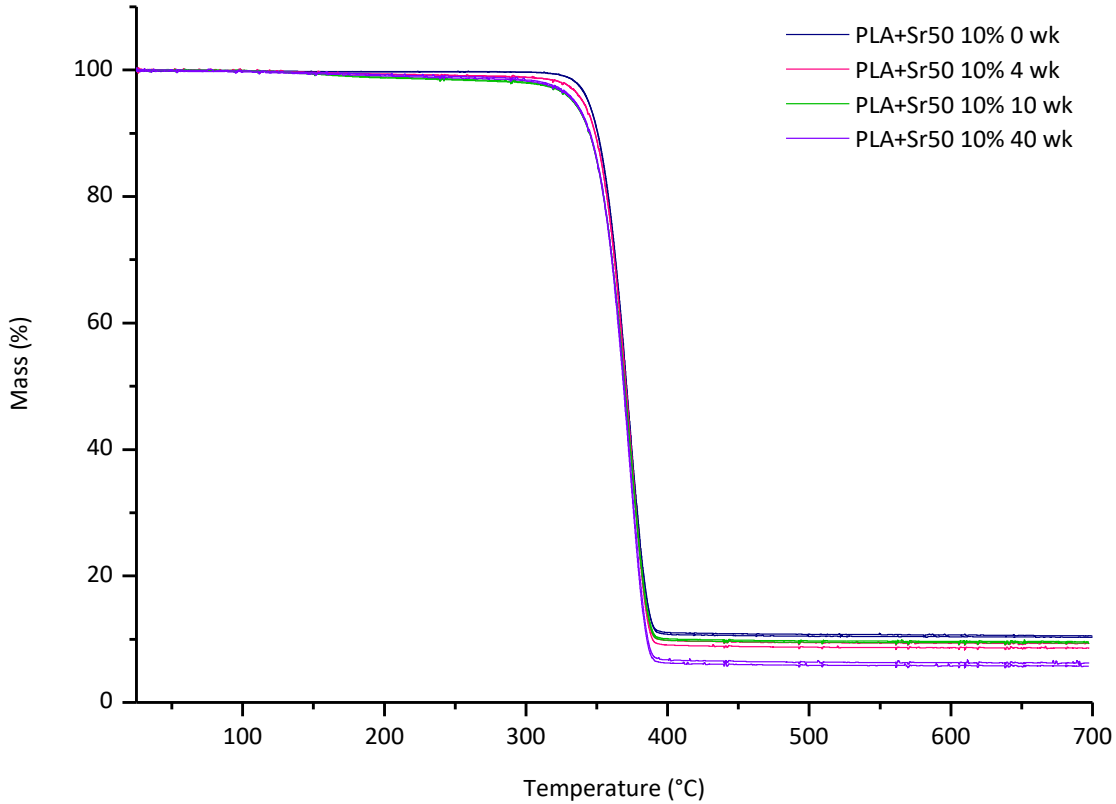

Figure B-4. *TGA graphs of PLA+Sr50 10% composite after 0, 4, 10, and 40 weeks of hydrolysis in TRIS at 37 °C. For each time point, two parallel measurements were done.*

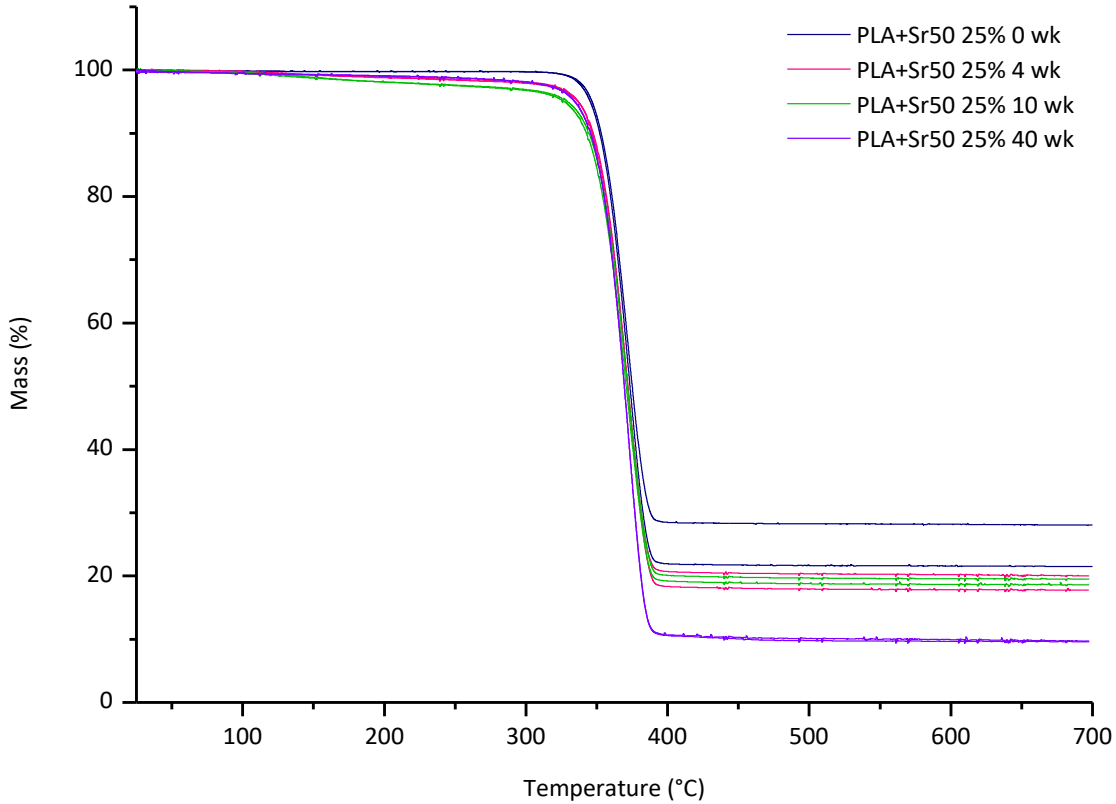

Figure B-5. *TGA graphs of PLA+Sr50 25% composite after 0, 4, 10, and 40 weeks of hydrolysis in TRIS at 37 °C. For each time point, two parallel measurements were done.*

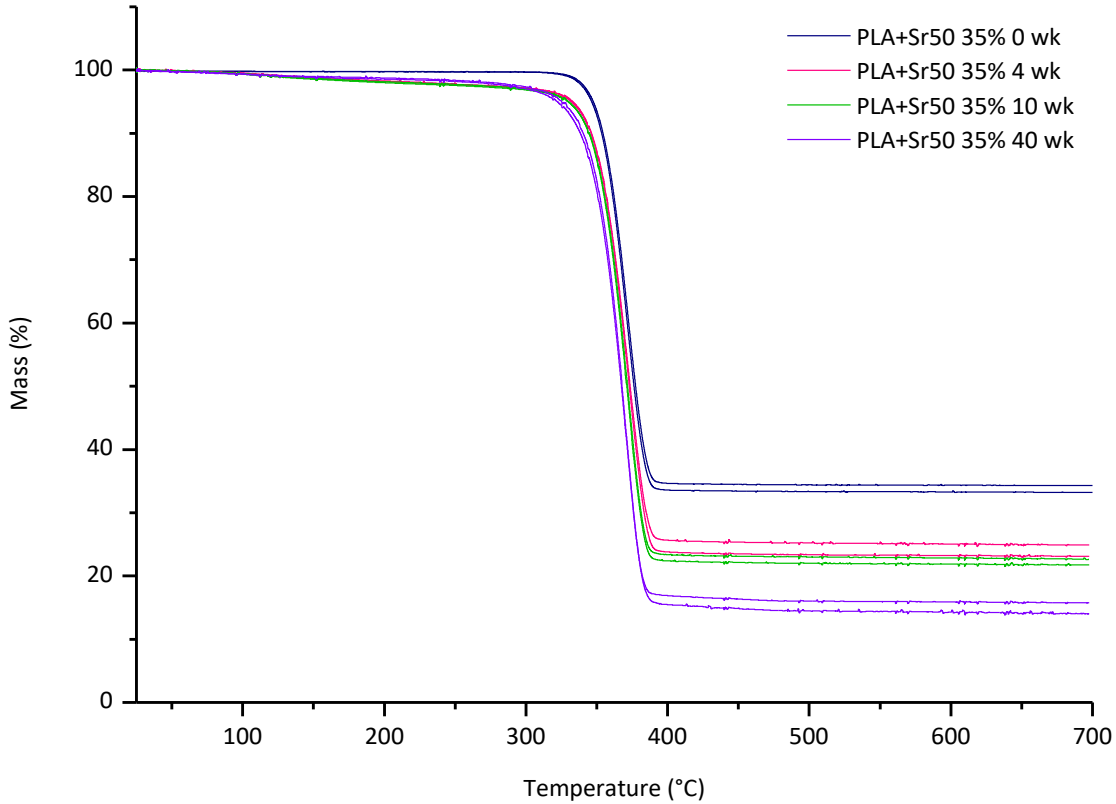

Figure B-6. *TGA graphs of PLA+Sr50 35% composite after 0, 4, 10, and 40 weeks of hydrolysis in TRIS at 37 °C. For each time point, two parallel measurements were done.*